

Supporting Information For:

A Fluorophore Anchored MOF for Fast and Sensitive Sensing of Cu(II) and 3-Nitrotyrosine in Physiological medium

*Srijan Mukherjee, Kabita Sarkar and Shyam Biswas**

Department of Chemistry, Indian Institute of Technology Guwahati, Guwahati, 781039 Assam, India.

* Corresponding author. Tel: 91-3612583309, fax: 91-3612582349.

E-mail address: sbiswas@iitg.ac.in.

1. Materials and Characterization Methods:

All the reagents and solvents were procured from commercial sources and used without purification, except the 2-((5-(dimethylamino)naphthalene)-1-sulfonamido) terephthalic acid linker.¹ The notations used for characterization of the bands are broad (br), strong (s), very strong (vs), medium (m), weak (w) and shoulder (sh). PXRD data were collected by using Rigaku Smartlab X-ray diffractometer with Cu-K α radiation ($\lambda = 1.54056 \text{ \AA}$), 50 kV of operating voltage and 100 mA of operating current. The Attenuated Total Reflectance Infrared (ATR-IR) spectra were recorded using PerkinElmer UATR Two at ambient condition in the region 400-4000 cm^{-1} . Thermogravimetric analysis (TGA) was carried out with a TG 209 F1 Libra Netzsch thermogravimetric analyzer in the temperature range of 25-700 $^{\circ}\text{C}$ in an N_2 atmosphere at the rate of 4 $^{\circ}\text{C min}^{-1}$. N_2 sorption isotherms were recorded by using Quantachrome Autosorb iQ-MP volumetric gas adsorption equipment at $-196 \text{ }^{\circ}\text{C}$. Before the sorption analysis, the degassing of the compound was carried out at 120 $^{\circ}\text{C}$ under a high vacuum for 12 h. Fluorescence sensing studies were performed with a HORIBA JOBIN YVON Fluoromax-4 spectrofluorometer. FE-SEM images were captured with a Zeiss (Zemini) scanning electron microscope. A Bruker Avance III 600 NMR spectrometer was used for recording ^1H NMR spectra at 500 MHz. Mass spectra were recorded with an Agilent 6520 QTOF high-resolution mass spectrometer (HR-MS). Fluorescence lifetimes were measured using Picosecond Time-resolved and Steady State Luminescence Spectrometer on an Edinburg Instruments Lifespec II & FSP 920 instrument. Pawley refinement was carried out using Materials Studio software. XPS measurement was performed with PHI-5000 Versaprobe III (ULVAC-PHI Inc.) photoelectron spectrometer.

2. Fluorescence detection of Cu(II) and 3-NTyr in human blood serum samples:

From the right arm vein of a completely healthy individual (blood group: A⁺), 10 mL of blood sample was taken out and centrifuged at 10000 rpm for 15 min to separate out the blood plasma. The pale-yellow coloured blood serum was collected in a falcon tube and kept in a refrigerator at $-20 \text{ }^{\circ}\text{C}$. For fluorescence detection experiments, aliquots of different concentrations of Cu(II) and 3-nitrotyrosine (3-NTyr) were spiked into the human blood serum sample, which contained HEPES buffer suspension of the probe.

3. Fluorescence detection of Cu(II) and 3-NTyr in human urine samples:

From a completely healthy individual, 10 mL of first early morning urine sample was collected and 500 μL of HNO_3 was poured into the sample to eliminate all the interfering living organisms. The sample was centrifuged at 8000 rpm for 10 min. The supernatants were taken for the experiments. For fluorescence detection experiments, different aliquots of Cu(II) and 3-NTyr were spiked in the urine sample containing HEPES buffer suspension of the probe.

4. Temperature dependent fluorescence study:

Temperature dependent study was carried out by following previously reported procedure in the literature.²

Equations used:

$$I_0/I = 1 + K_{SV}[Q] \quad (1)$$

$$\log\left(\frac{I_0 - I}{I}\right) = \log K_a + n \log[Q] \quad (2)$$

$$\log(K_a) = -\frac{\Delta H}{RT} + \frac{\Delta S}{R} \quad (3)$$

$$\Delta G = \Delta H - T\Delta S \quad (4)$$

I_0 = Initial fluorescence intensity, I = final fluorescence intensity, Q = concentration of analyte, K_{SV} = S-V quenching constant, K_a = binding energy at corresponding temperature, n = binding site, T = temperature, R = universal gas constant, ΔG = change in Gibbs free energy, ΔH = Change in enthalpy, ΔS = change in entropy.

K_{SV} value at different temperature was determined from equation no 1 and by plotting I_0/I vs. concentration. Further binding constant at different temperature was determined by plotting $\log\left(\frac{I_0 - I}{I}\right)$ vs $\log[Q]$ and equation 2 is utilized. All other thermodynamic terms are determined from van't Hoff plot and utilizing equations 3 and 4.

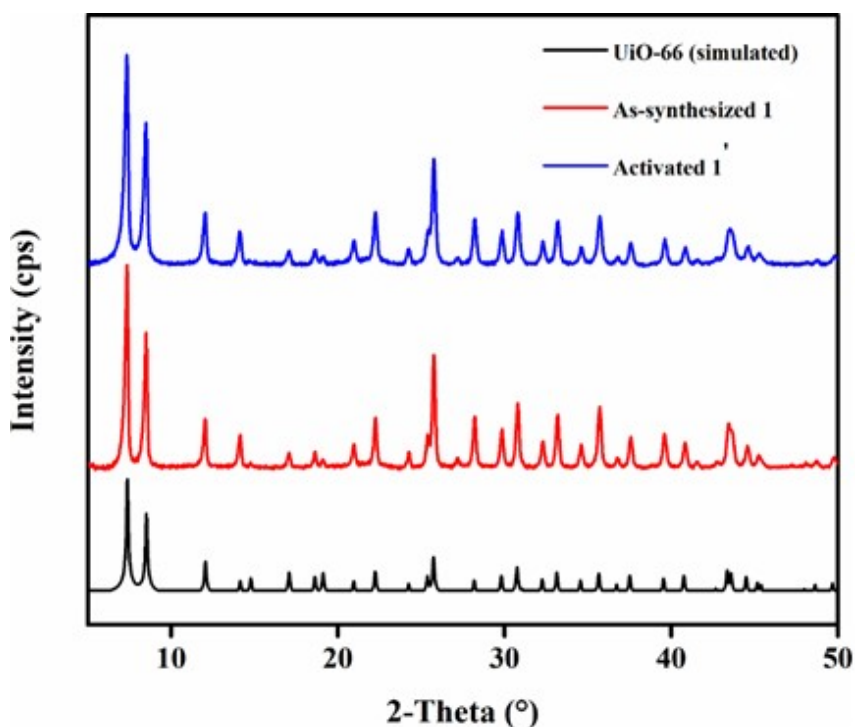


Figure S1. PXRD patterns of simulated **UiO-66** (black), as-synthesized **1** (red), activated **1'** (blue).

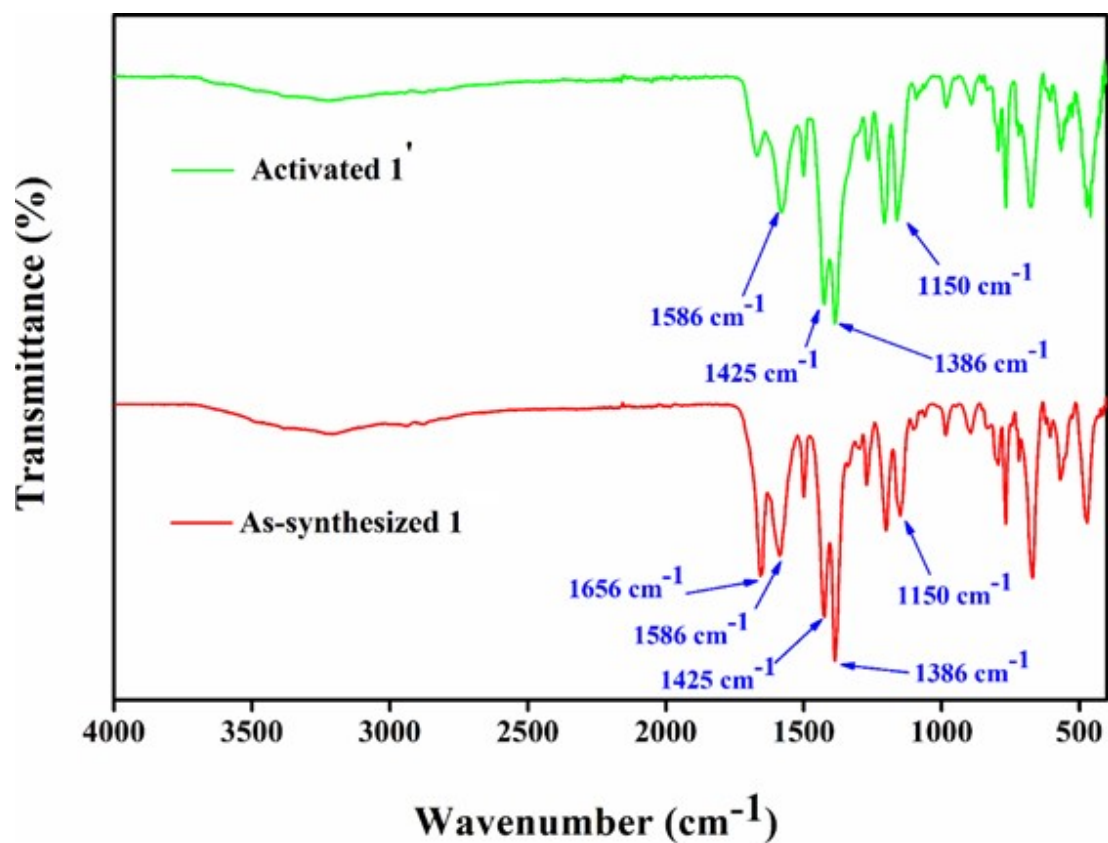


Figure S2. IR spectra of as-synthesized **1** and activated **1'**.

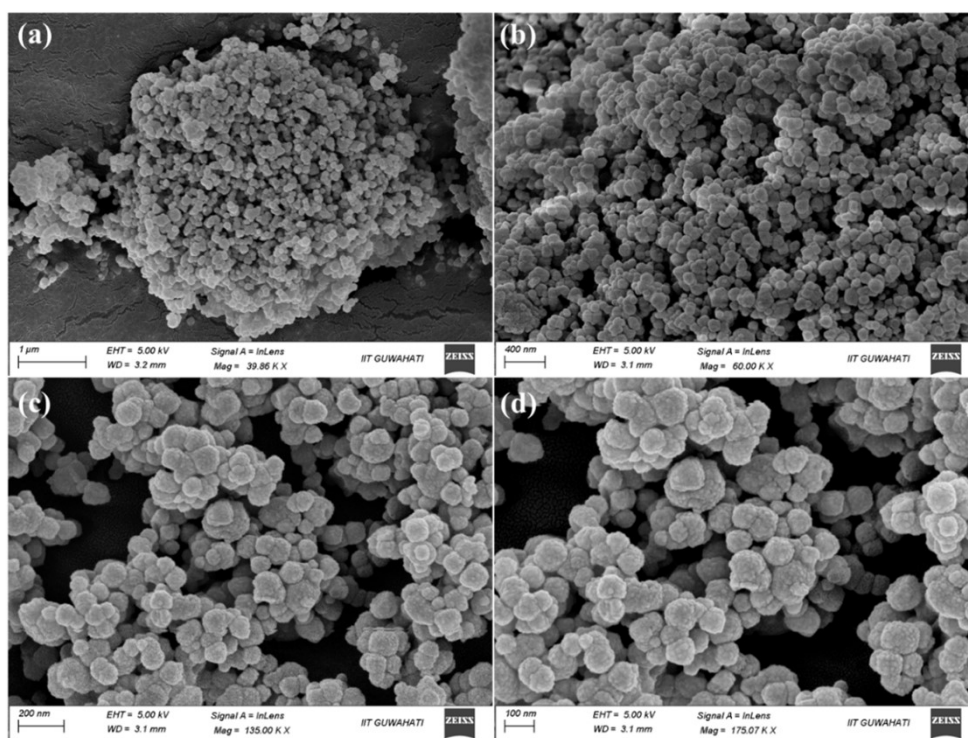


Figure S3. FE-SEM images of **1'** under different magnifications.

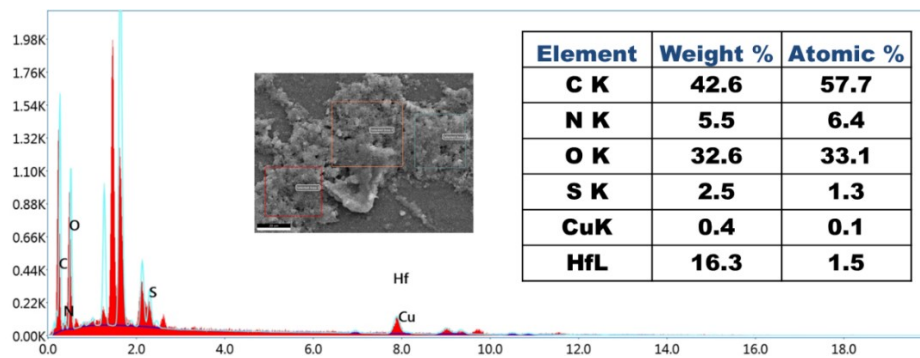


Figure S4. EDX spectrum of 1'.

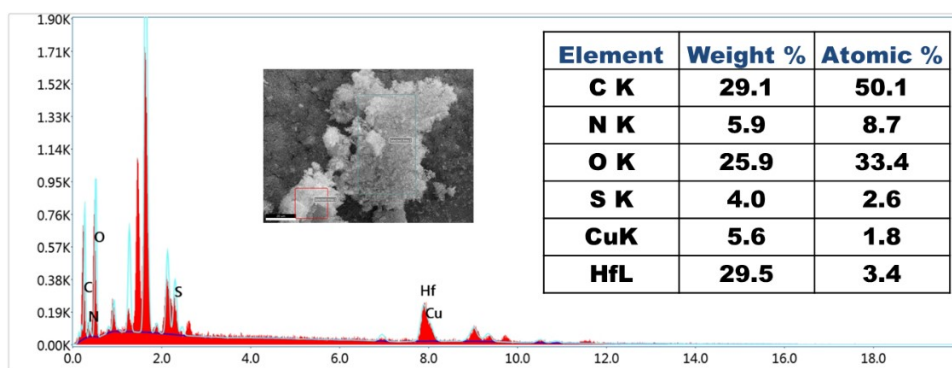


Figure S5. EDX spectrum of 1' after Cu²⁺ treatment.

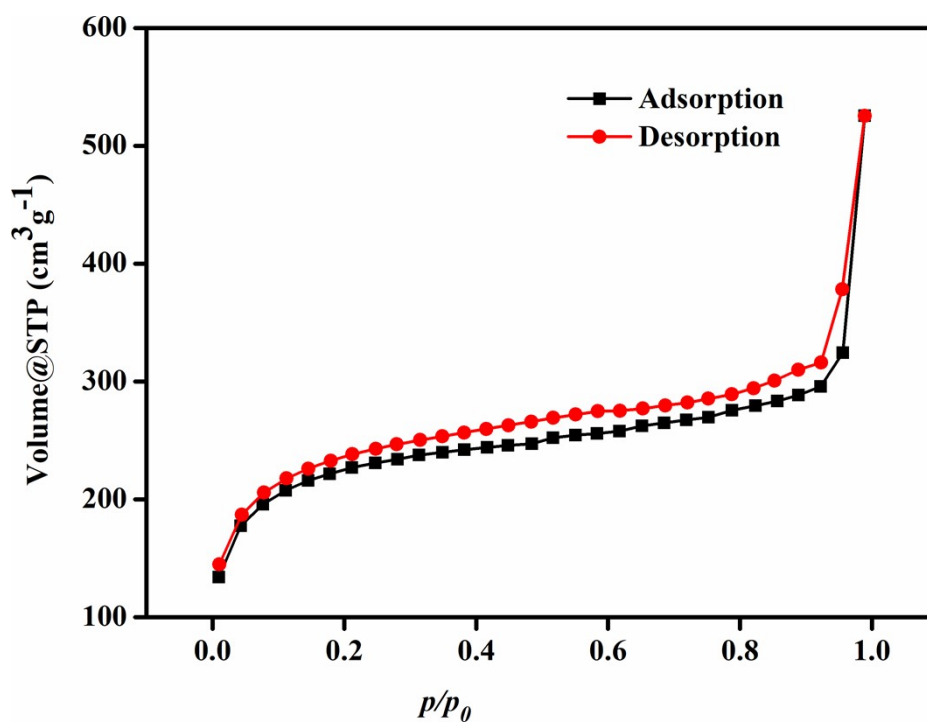


Figure S6. N₂ sorption isotherms of activated 1' (recorded at -196 °C).

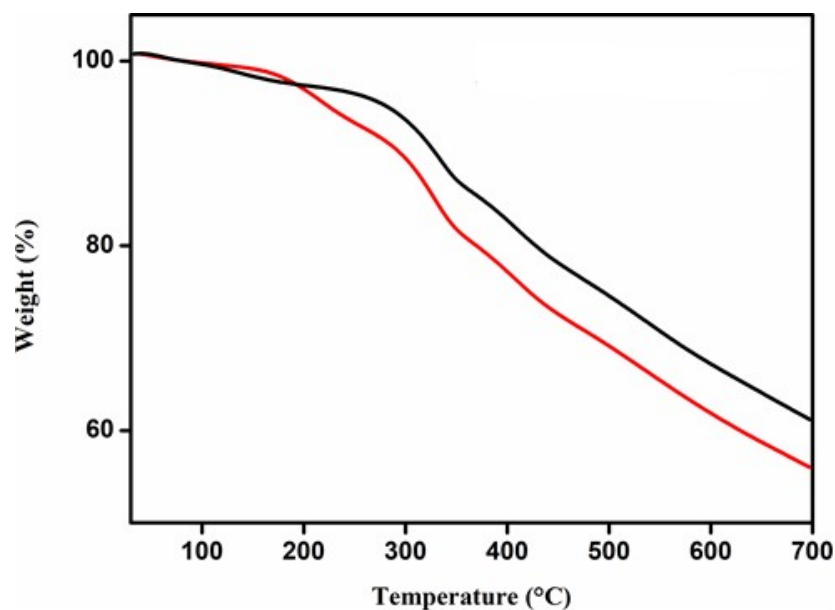


Figure S7. TGA curves of as-synthesized **1** (red), activated **1'** (black) recorded in the temperature range of 30-700 °C with a heating rate of 4 °C min⁻¹ in N₂ atmosphere.

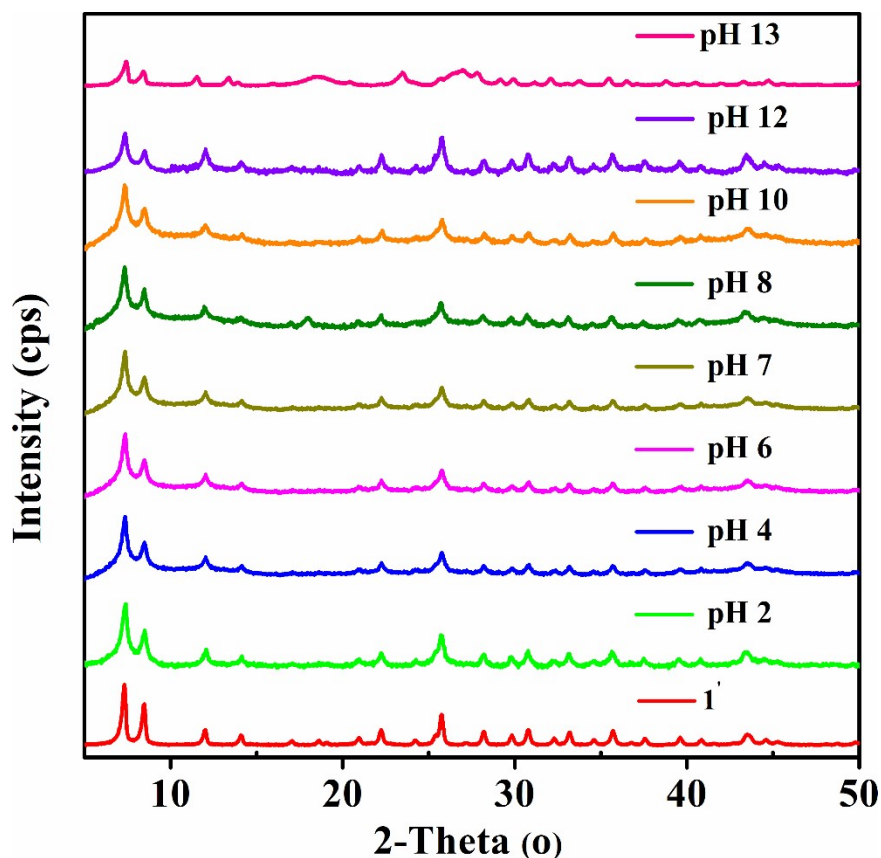


Figure S8. PXRD patterns of **1'** (red), after stirring in pH 2 (green), pH 4 (dark blue), pH 6 (purple), pH 7 (olive green), pH 8 (green), pH 10 (orange), pH 12 (violet) and pH 13 (pink) solutions.

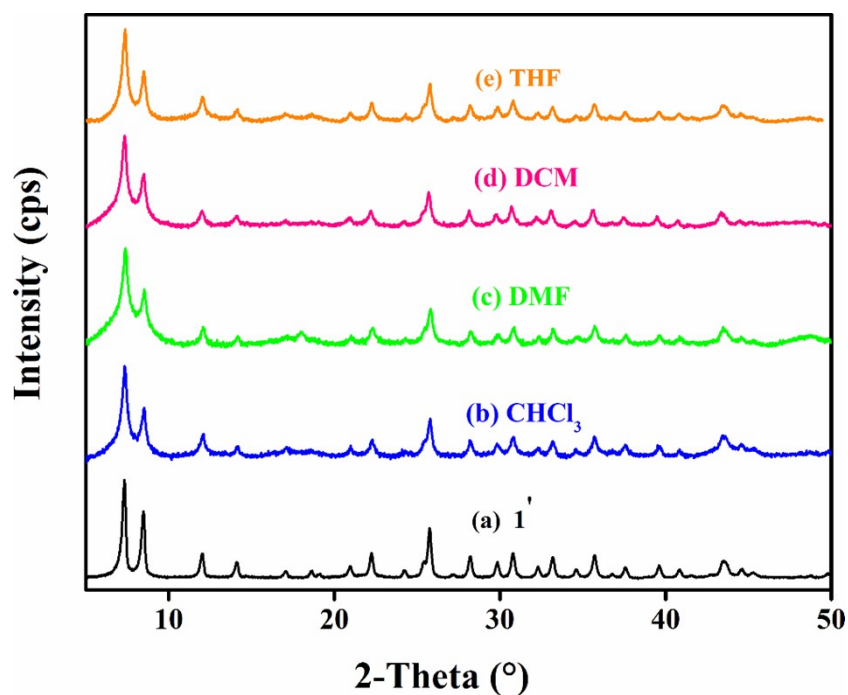


Figure S9. PXRD patterns of (a) activated **1'** (black), after stirring in (b) CHCl₃ (blue), (c) DMF (green), (d) DCM (pink) and (e) THF (orange) solutions.

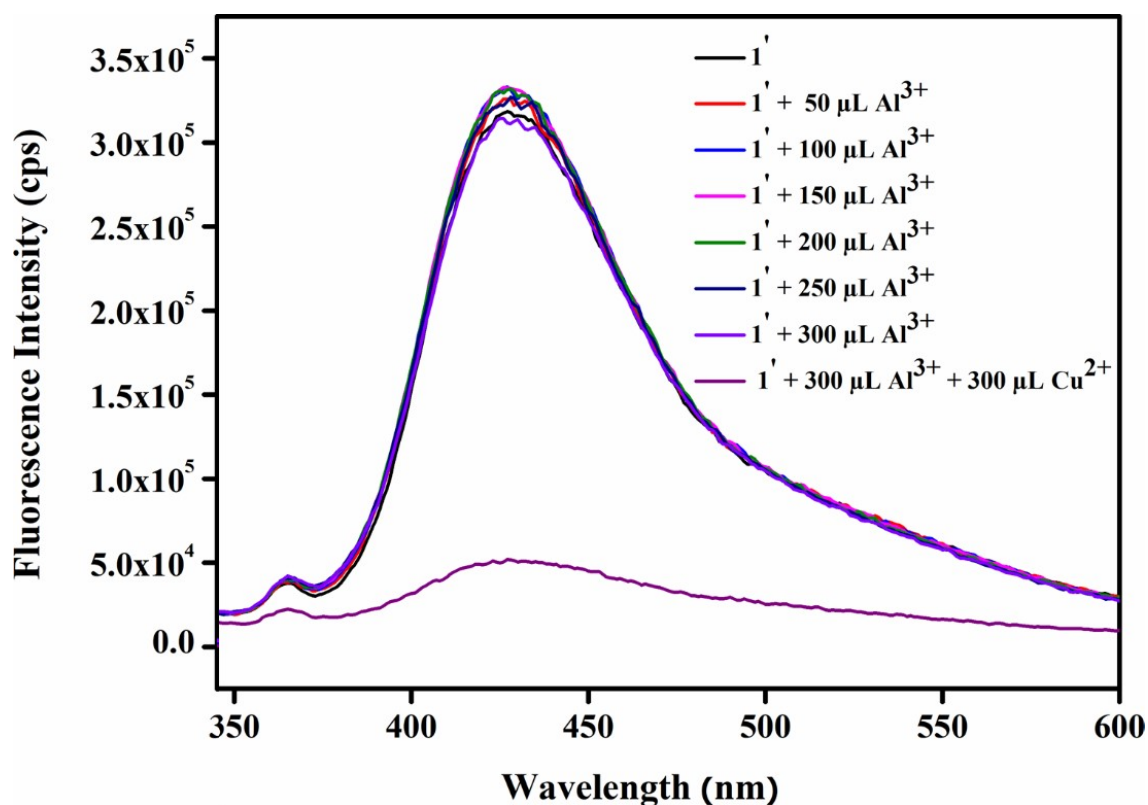


Figure S10. Change in fluorescence emission intensity of activated **1'** (in HEPES medium) upon addition of 300 μL of 10 mM Cu²⁺ in presence of 300 μL of 10 mM Al³⁺ solution ($\lambda_{\text{ex}} = 325$ nm and $\lambda_{\text{em}} = 428$ nm).

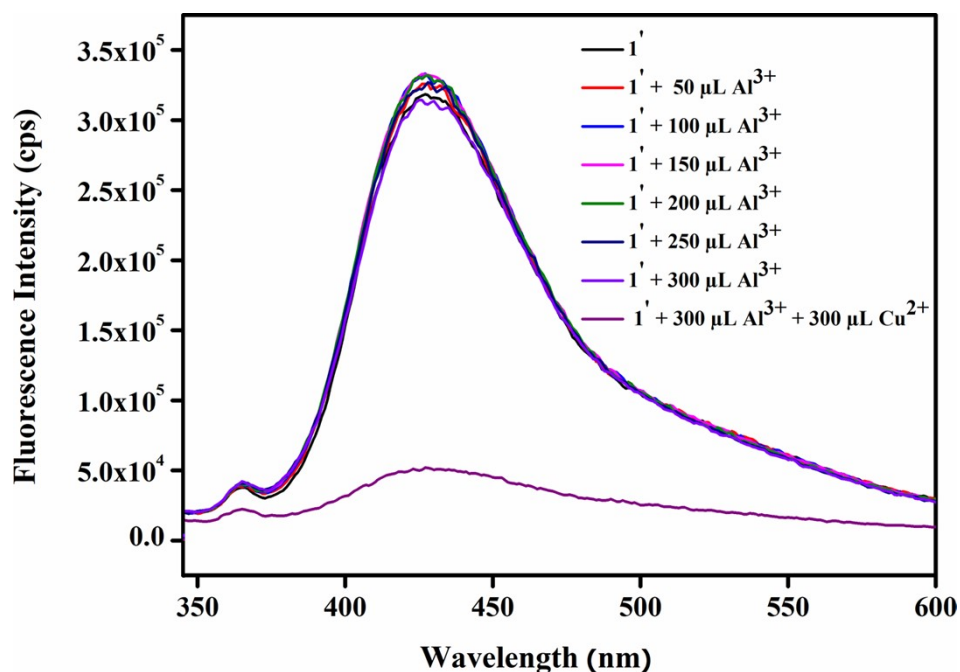


Figure S11. Change in fluorescence emission intensity of activated $1'$ (in HEPES medium) upon addition of 300 μL of 10 mM Cu^{2+} in presence of 300 μL of 10 mM Ca^{2+} solution ($\lambda_{\text{ex}} = 325$ nm and $\lambda_{\text{em}} = 428$ nm).

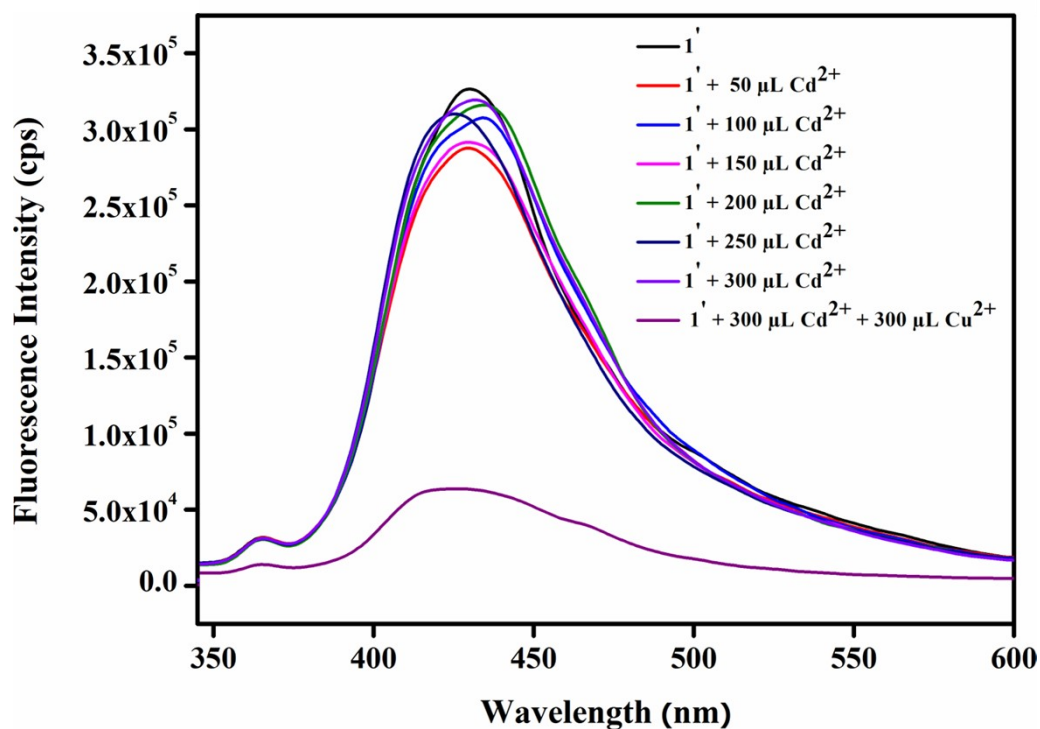


Figure S12. Change in fluorescence emission intensity of activated $1'$ (in HEPES medium) upon addition of 300 μL of 10 mM Cu^{2+} in presence of 300 μL of 10 mM Cd^{2+} solution ($\lambda_{\text{ex}} = 325$ nm and $\lambda_{\text{em}} = 428$ nm).

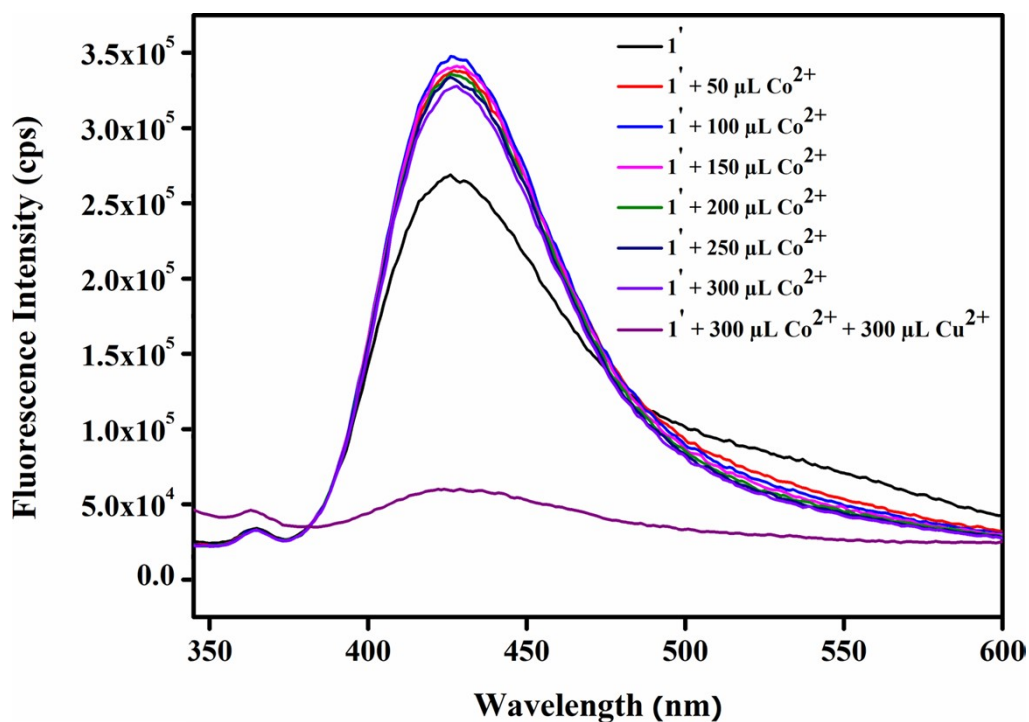


Figure S13. Change in fluorescence emission intensity of activated $1'$ (in HEPES medium) upon addition of 300 μL of 10 mM Cu^{2+} in presence of 300 μL of 10 mM Co^{2+} solution ($\lambda_{\text{ex}} = 325$ nm and $\lambda_{\text{em}} = 428$ nm).

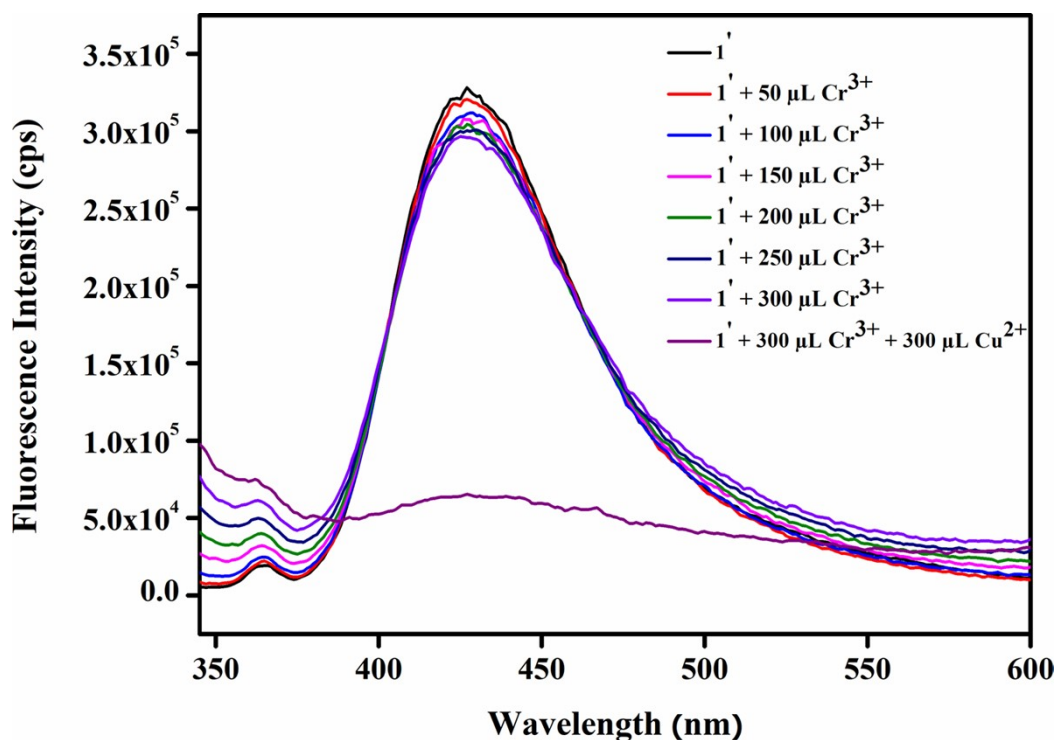


Figure S14. Change in fluorescence emission intensity of activated $1'$ (in HEPES medium) upon addition of 300 μL of 10 mM Cu^{2+} in presence of 300 μL of 10 mM Cr^{3+} solution ($\lambda_{\text{ex}} = 325$ nm and $\lambda_{\text{em}} = 428$ nm).

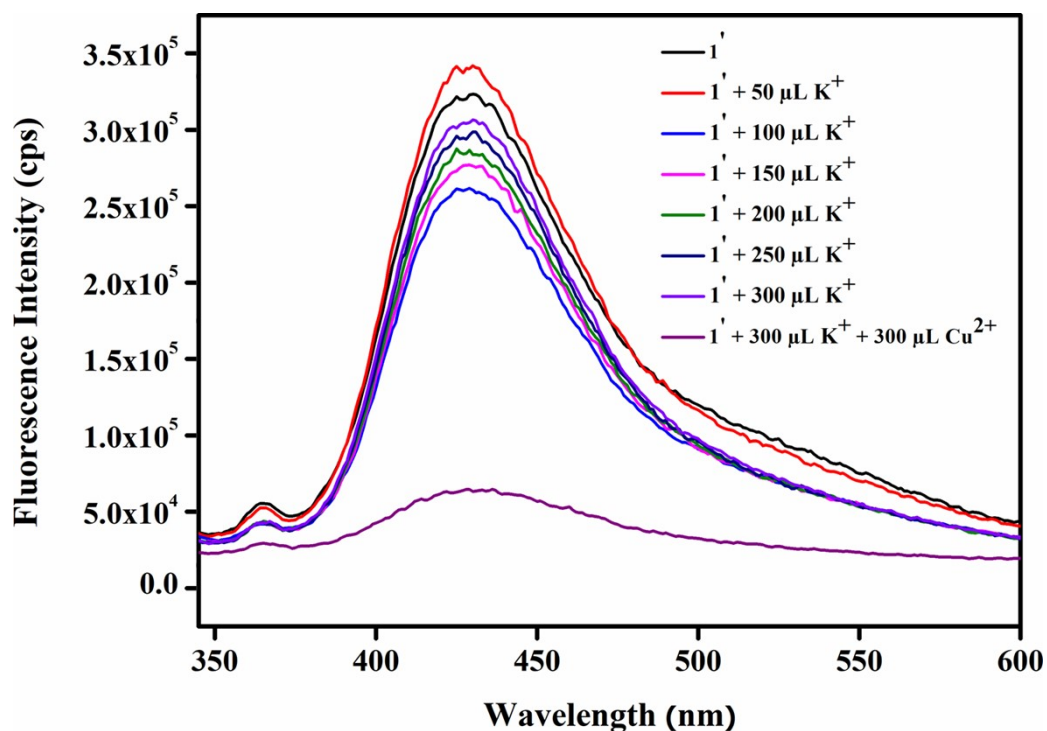


Figure S15. Change in fluorescence emission intensity of activated $1'$ (in HEPES medium) upon addition of $300 \mu\text{L}$ of 10 mM Cu^{2+} in presence of $300 \mu\text{L}$ of 10 mM K^+ solution ($\lambda_{\text{ex}} = 325 \text{ nm}$ and $\lambda_{\text{em}} = 428 \text{ nm}$).

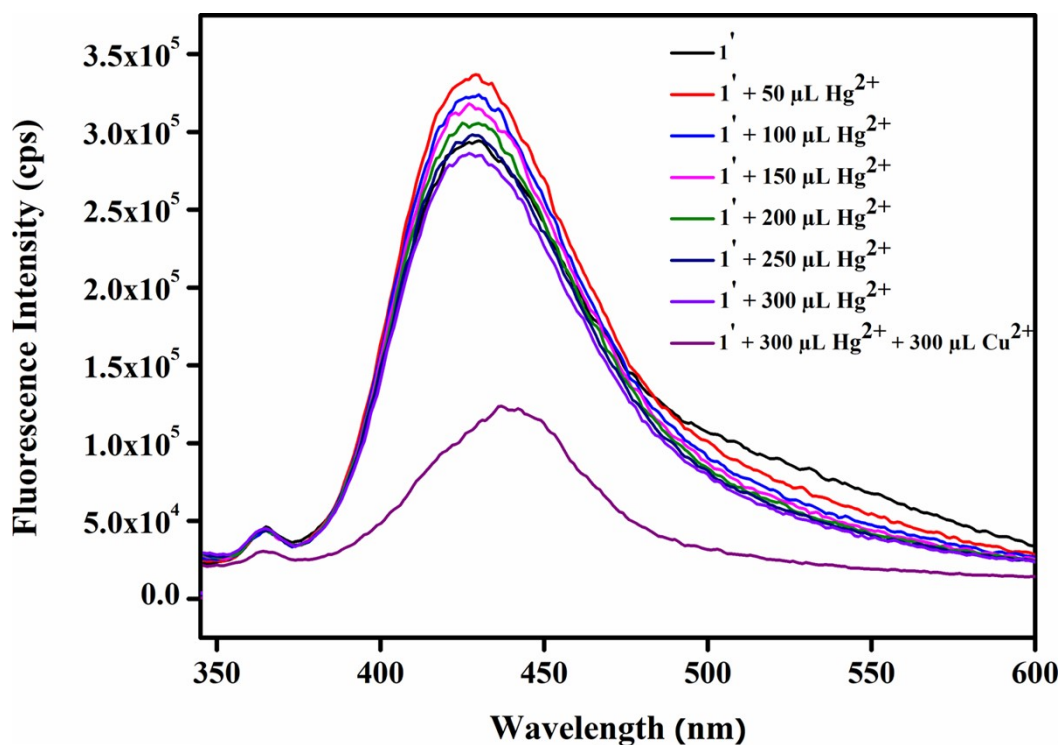


Figure S16. Change in fluorescence emission intensity of activated $1'$ (in HEPES medium) upon addition of $300 \mu\text{L}$ of 10 mM Cu^{2+} in presence of $300 \mu\text{L}$ of 10 mM Hg^{2+} solution ($\lambda_{\text{ex}} = 325 \text{ nm}$ and $\lambda_{\text{em}} = 428 \text{ nm}$).

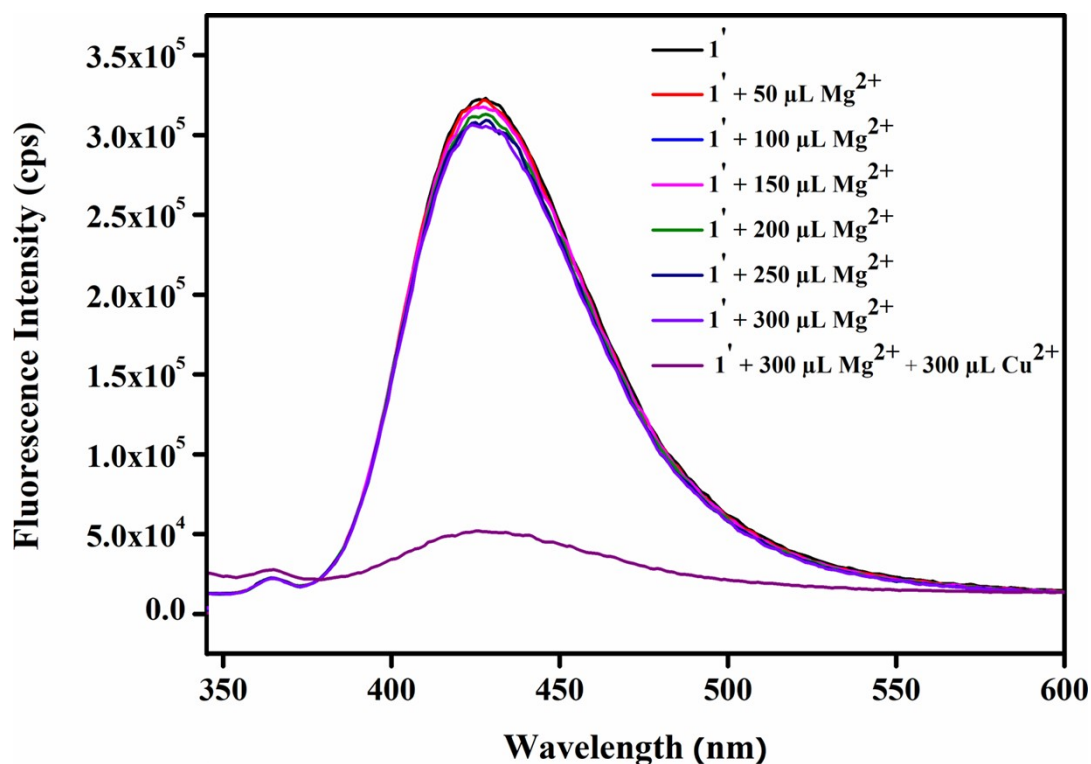


Figure S17. Change in fluorescence emission intensity of activated $1'$ (in HEPES medium) upon addition of 300 μL of 10 mM Cu^{2+} in presence of 300 μL of 10 mM Mg^{2+} solution ($\lambda_{\text{ex}} = 325$ nm and $\lambda_{\text{em}} = 428$ nm).

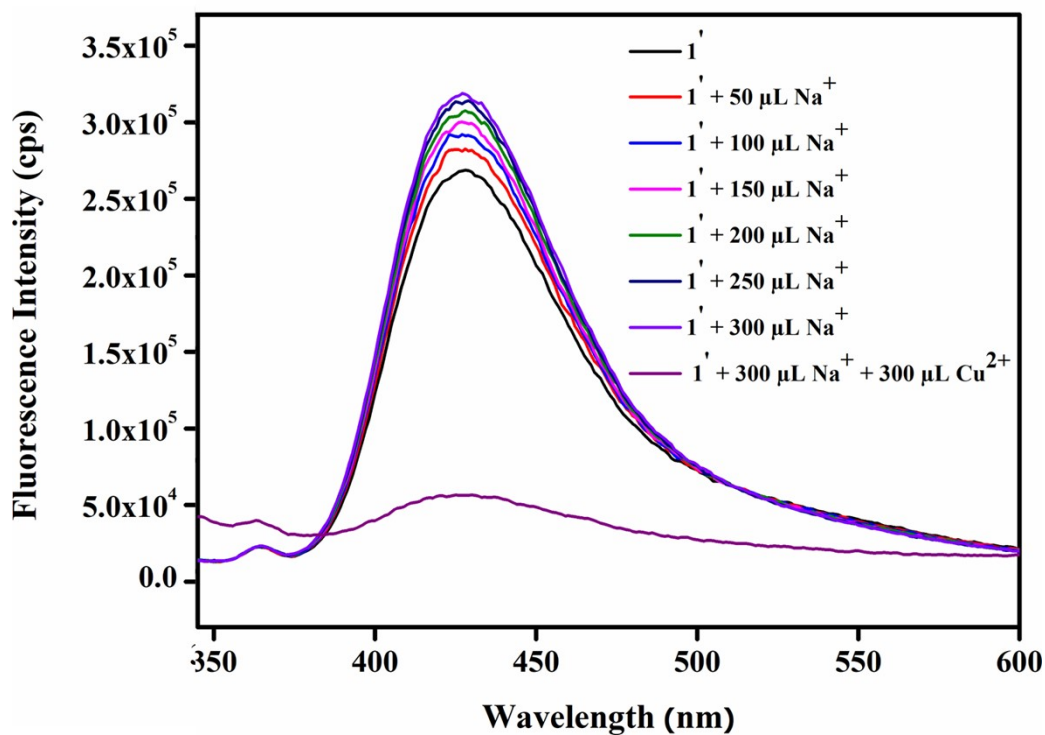


Figure S18. Change in fluorescence emission intensity of activated $1'$ (in HEPES medium) upon addition of 300 μL of 10 mM Cu^{2+} in presence of 300 μL of 10 mM Na^+ solution ($\lambda_{\text{ex}} = 325$ nm and $\lambda_{\text{em}} = 428$ nm).

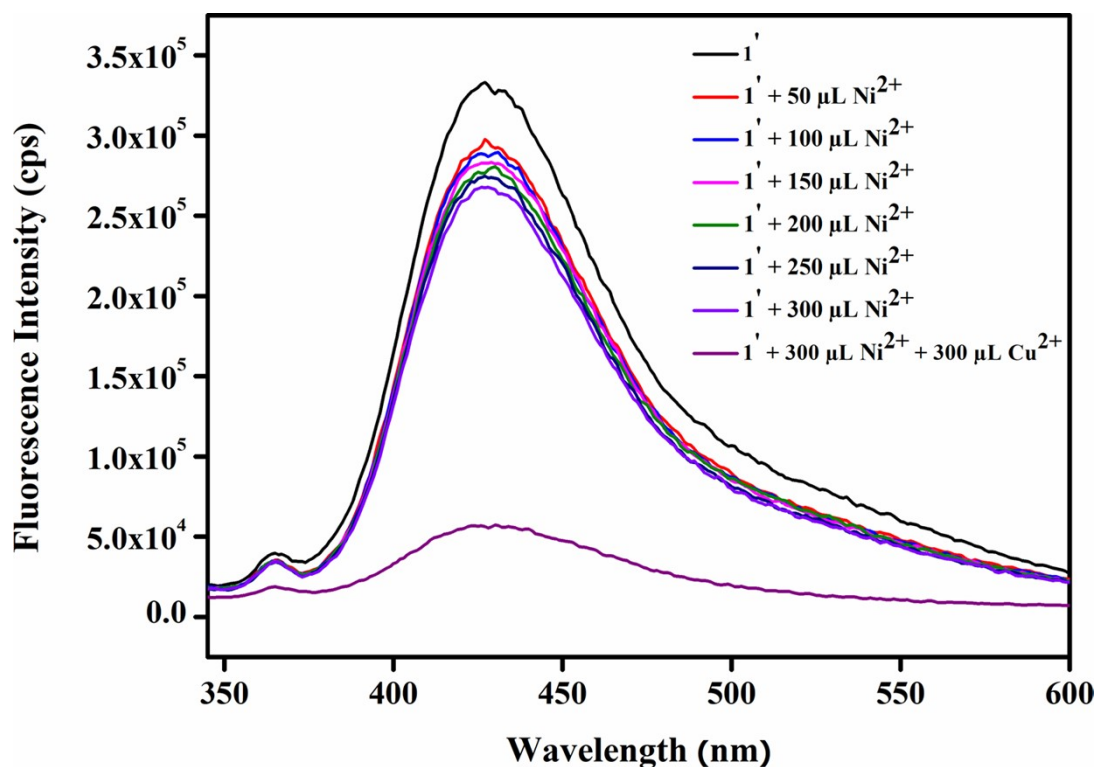


Figure S19. Change in fluorescence emission intensity of activated $1'$ (in HEPES medium) upon addition of 300 μL of 10 mM Cu^{2+} in presence of 300 μL of 10 mM Ni^{2+} solution ($\lambda_{\text{ex}} = 325$ nm and $\lambda_{\text{em}} = 428$ nm).

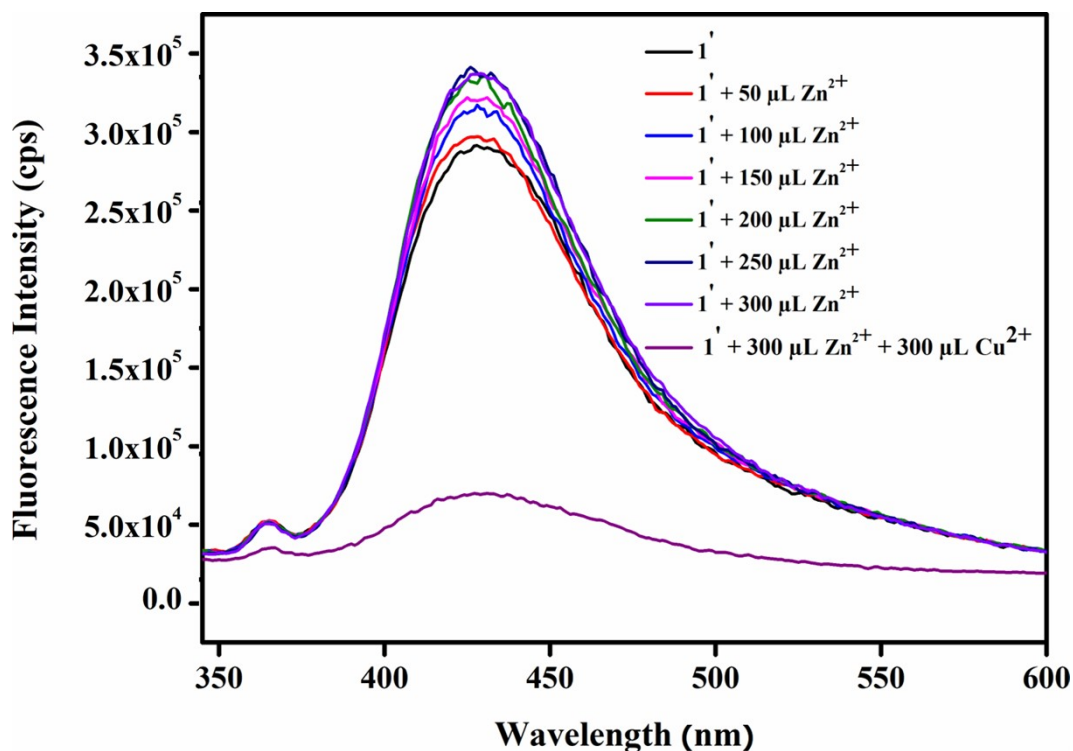


Figure S20. Change in fluorescence emission intensity of activated $1'$ (in HEPES medium) upon addition of 300 μL of 10 mM Cu^{2+} in presence of 300 μL of 10 mM Mg^{2+} solution ($\lambda_{\text{ex}} = 325$ nm and $\lambda_{\text{em}} = 428$ nm).

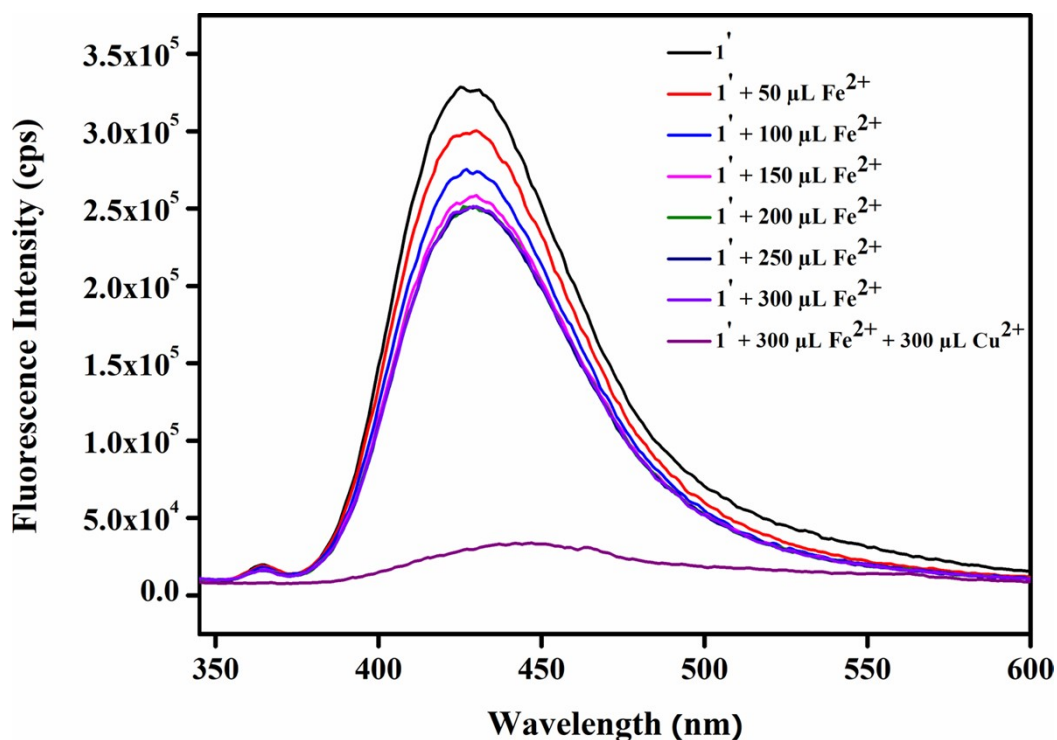


Figure S21. Change in fluorescence emission intensity of activated $1'$ (in HEPES medium) upon addition of 300 μL of 10 mM Cu^{2+} in presence of 300 μL of 10 mM Fe^{2+} solution ($\lambda_{\text{ex}} = 325$ nm and $\lambda_{\text{em}} = 428$ nm).

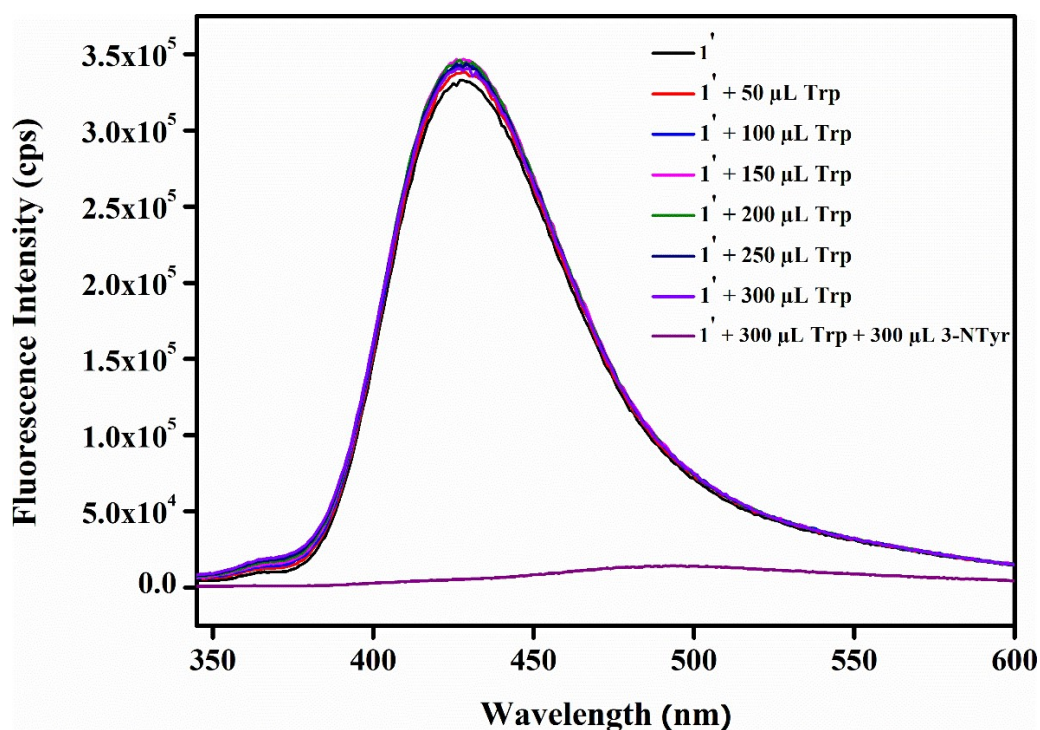


Figure S22. Change in fluorescence emission intensity of activated $1'$ (in HEPES medium) upon addition of 300 μL of 10 mM 3-NTyr in presence of 300 μL of 10 mM tryptophan (Trp) solution ($\lambda_{\text{ex}} = 325$ nm and $\lambda_{\text{em}} = 428$ nm).

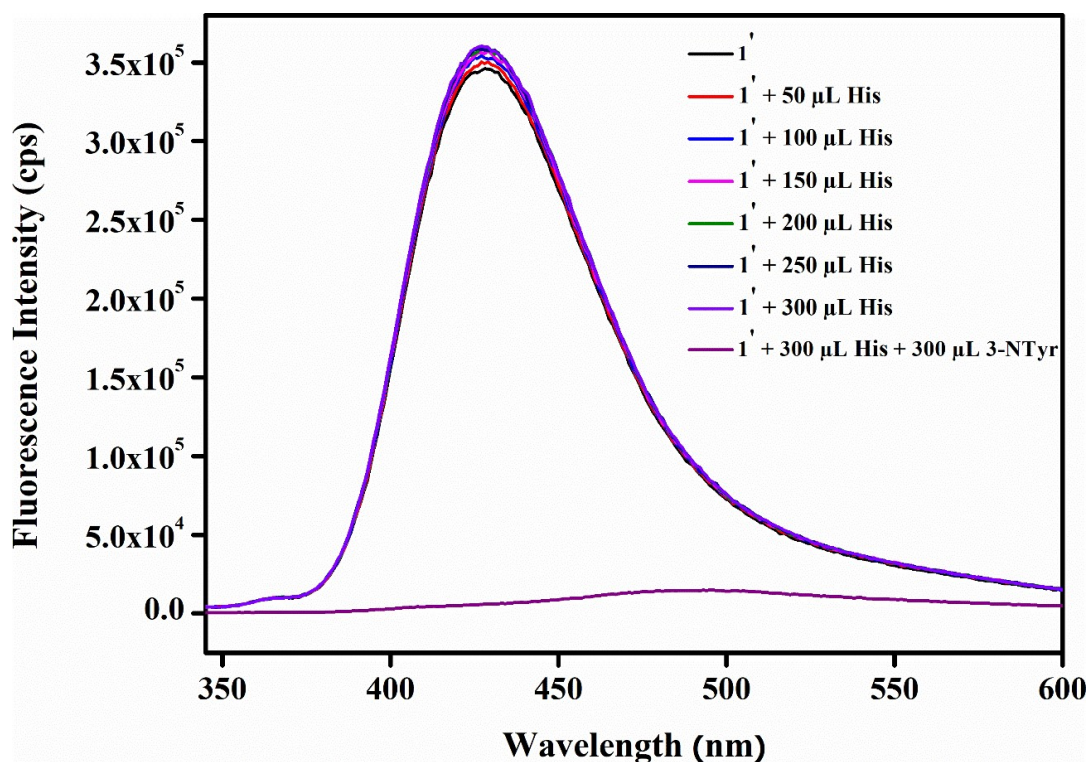


Figure S23. Change in fluorescence emission intensity of activated $1'$ (in HEPES medium) upon addition of 300 μ L of 10 mM 3-NTyr in presence of 300 μ L of 10 mM histidine (His) solution ($\lambda_{\text{ex}} = 325$ nm and $\lambda_{\text{em}} = 428$ nm).

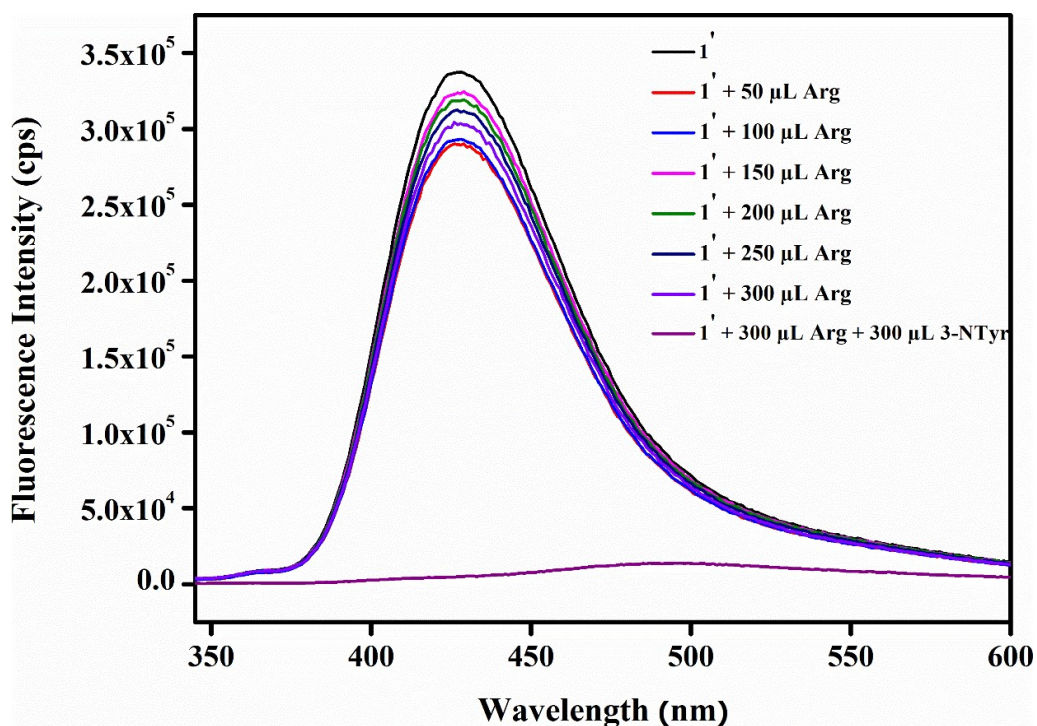


Figure S24. Change in fluorescence emission intensity of activated $1'$ (in HEPES medium) upon addition of 300 μ L of 10 mM 3-NTyr in presence of 300 μ L of 10 mM arginine (Arg) solution ($\lambda_{\text{ex}} = 325$ nm and $\lambda_{\text{em}} = 428$ nm).

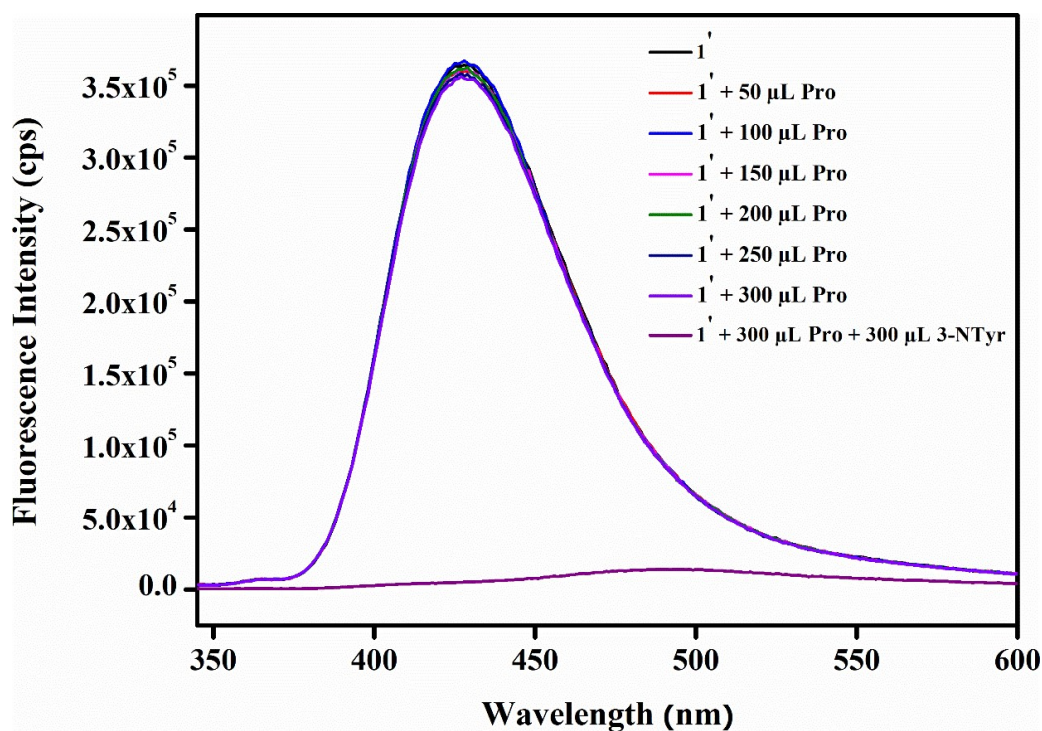


Figure S25. Change in fluorescence emission intensity of activated $1'$ (in HEPES medium) upon addition of 300 μL of 10 mM 3-NTyr in presence of 300 μL of 10 mM proline (Pro) solution ($\lambda_{\text{ex}} = 325 \text{ nm}$ and $\lambda_{\text{em}} = 428 \text{ nm}$).

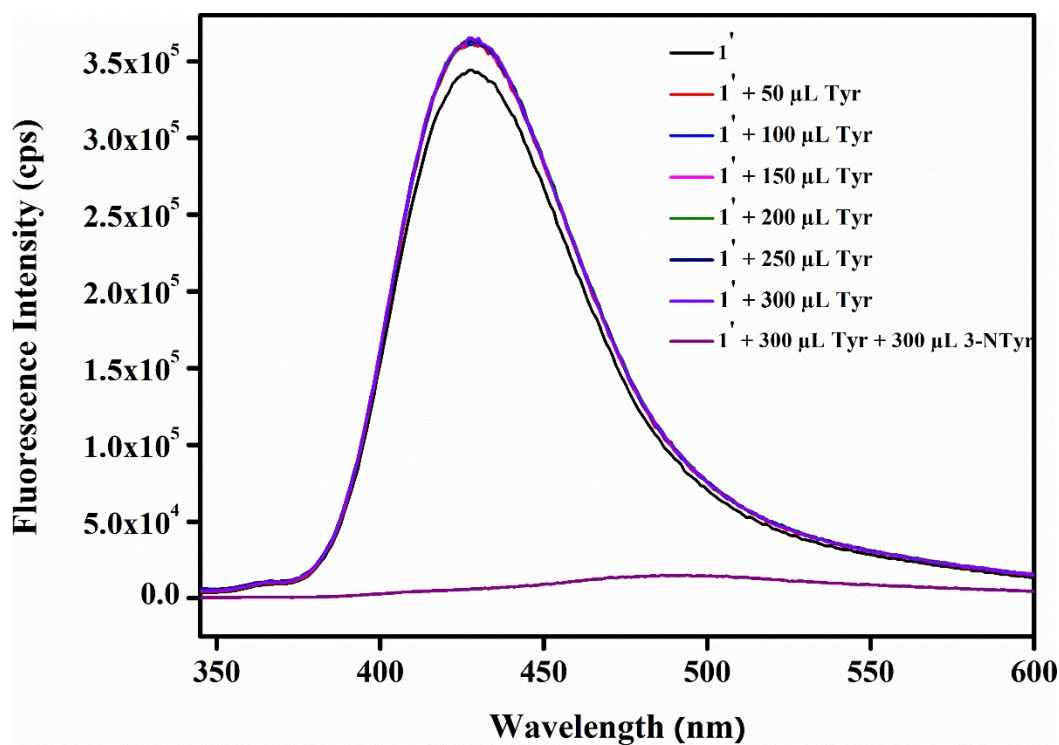


Figure S26. Change in fluorescence emission intensity of activated $1'$ (in HEPES medium) upon addition of 300 μL of 10 mM 3-NTyr in presence of 300 μL of 10 mM tyrosine (Tyr) solution ($\lambda_{\text{ex}} = 325 \text{ nm}$ and $\lambda_{\text{em}} = 428 \text{ nm}$).

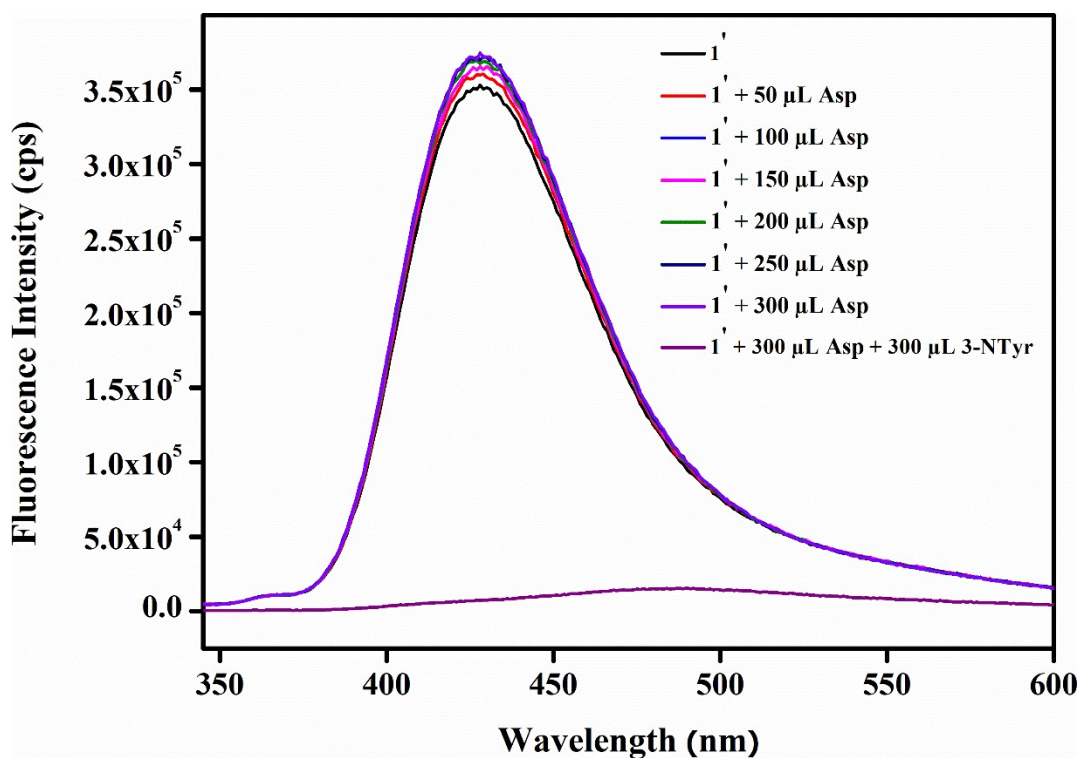


Figure S27. Change in fluorescence emission intensity of activated $1'$ (in HEPES medium) upon addition of 300 μL of 10 mM 3-NTyr in presence of 300 μL of 10 mM aspartic acid (Asp) solution ($\lambda_{\text{ex}} = 325 \text{ nm}$ and $\lambda_{\text{em}} = 428 \text{ nm}$).

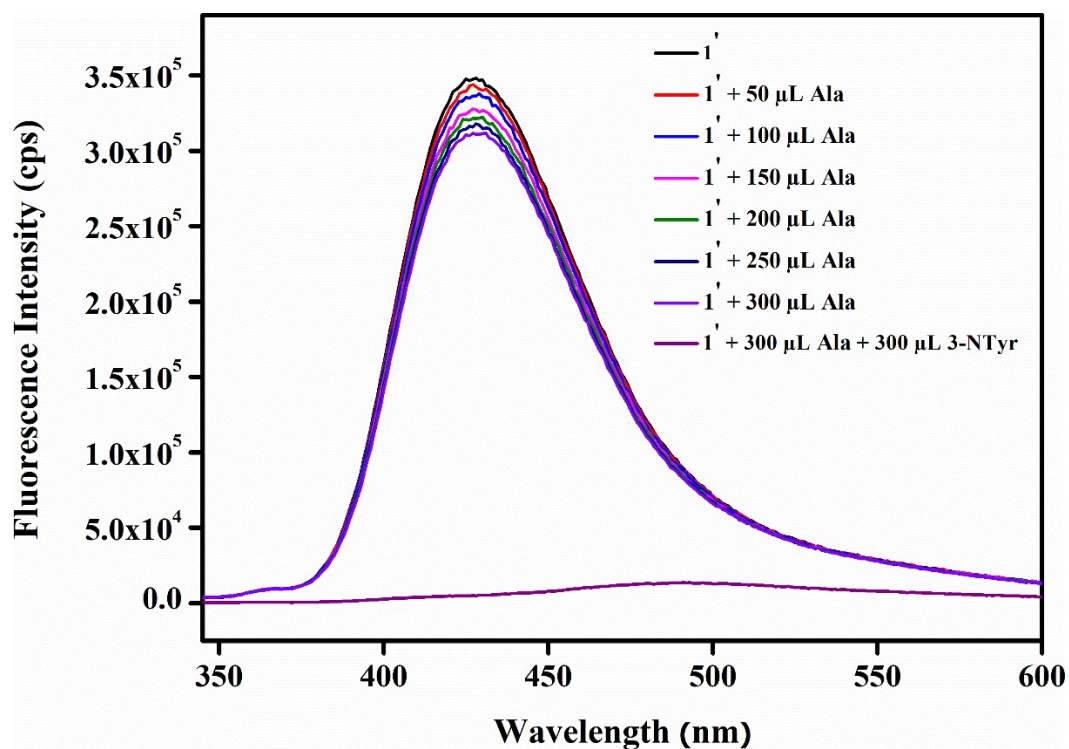


Figure S28. Change in fluorescence emission intensity of activated $1'$ (in HEPES medium) upon addition of 300 μL of 10 mM 3-NTyr in presence of 300 μL of 10 mM Alanine (Ala) solution ($\lambda_{\text{ex}} = 325 \text{ nm}$ and $\lambda_{\text{em}} = 428 \text{ nm}$).

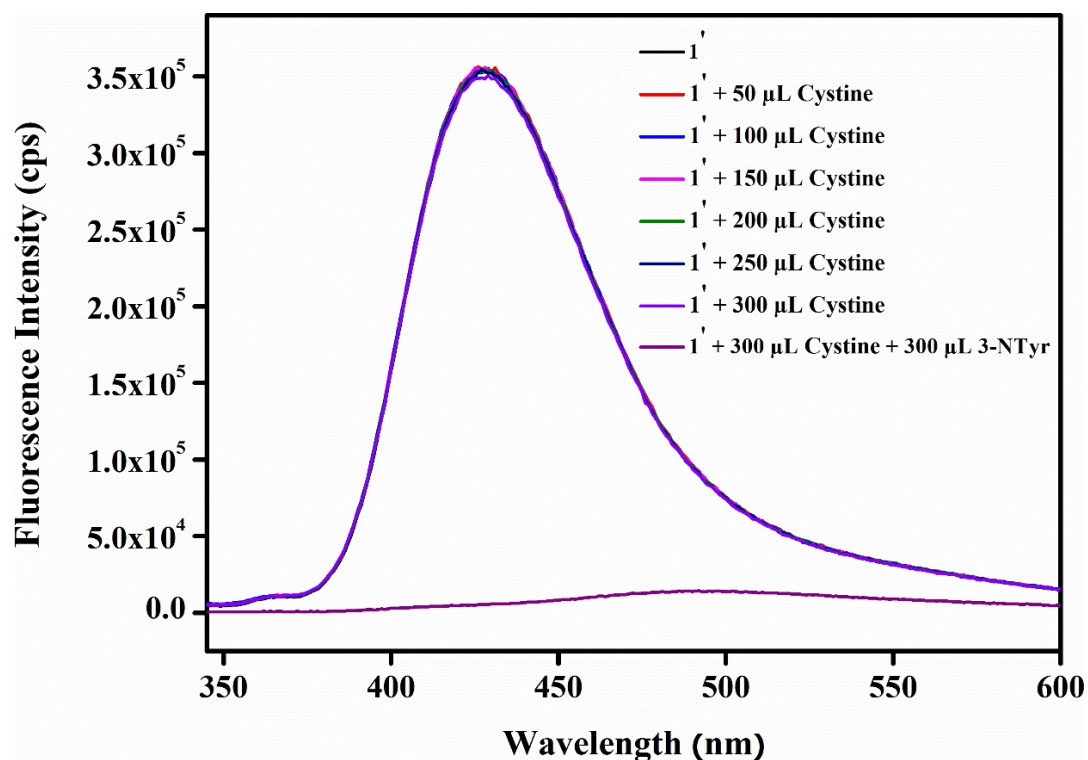


Figure S29. Change in fluorescence emission intensity of activated $1'$ (in HEPES medium) upon addition of 300 μL of 10 mM 3-NTyr in presence of 300 μL of 10 mM cysteine solution ($\lambda_{\text{ex}} = 325 \text{ nm}$ and $\lambda_{\text{em}} = 428 \text{ nm}$).

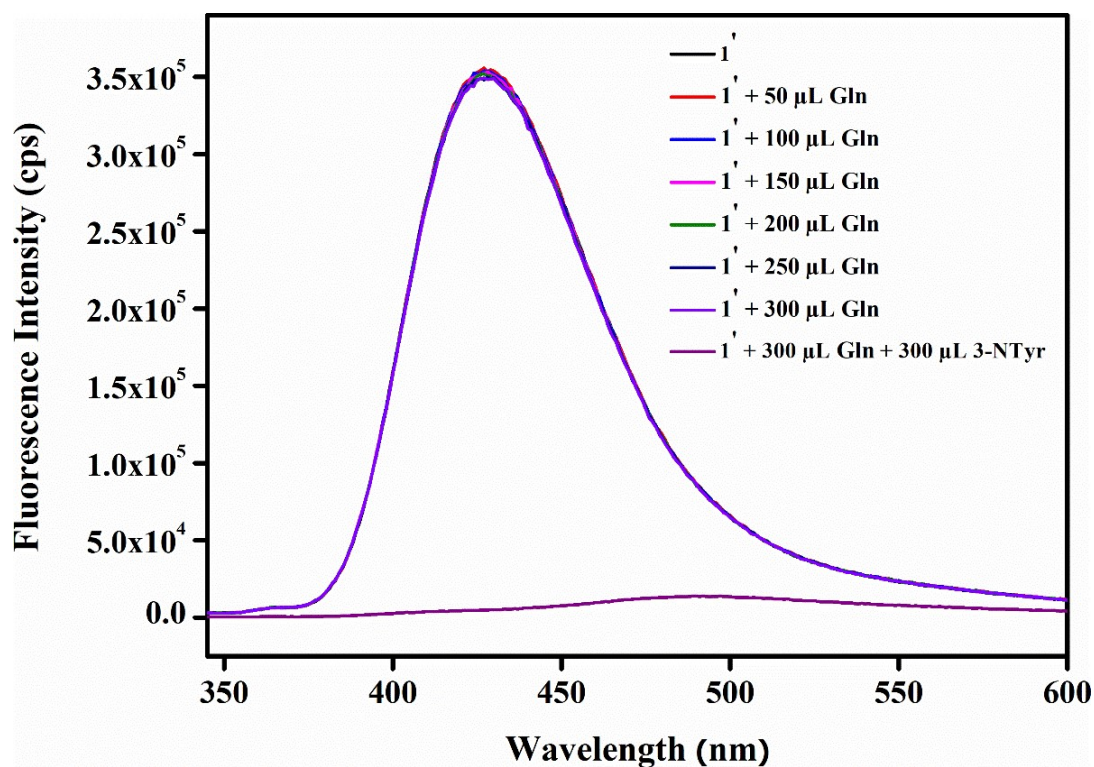


Figure S30. Change in fluorescence emission intensity of activated $1'$ (in HEPES medium) upon addition of 300 μL of 10 mM 3-NTyr in presence of 300 μL of 10 mM glutamine (Gln) solution ($\lambda_{\text{ex}} = 325 \text{ nm}$ and $\lambda_{\text{em}} = 428 \text{ nm}$).

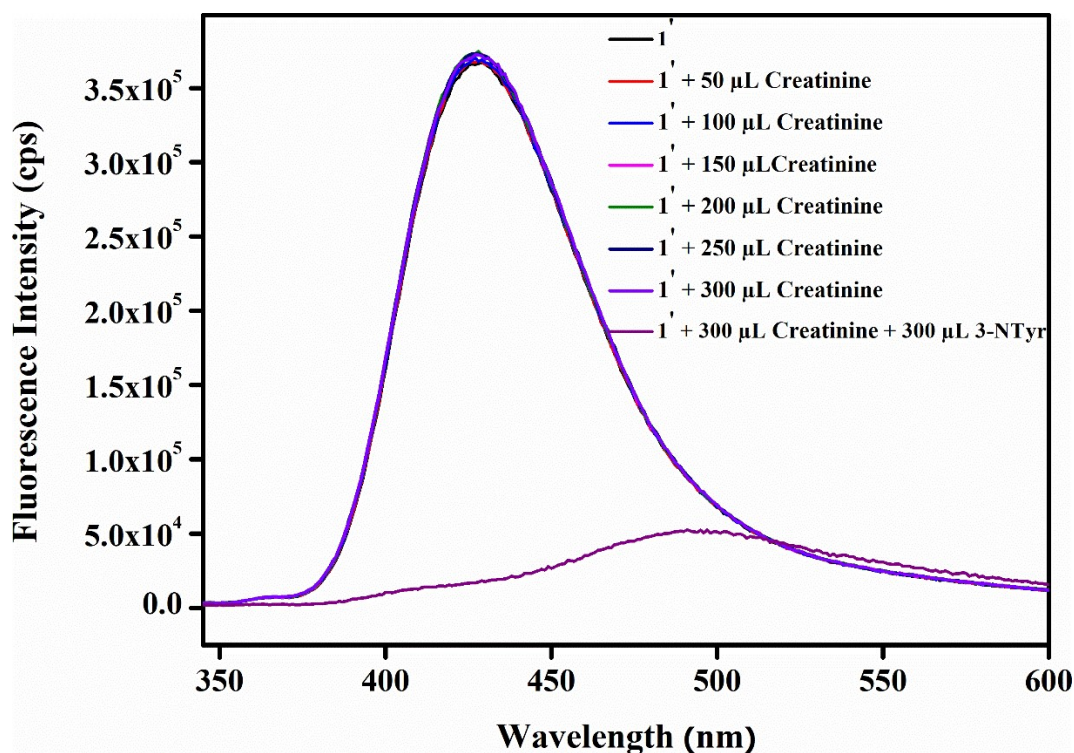


Figure S31. Change in fluorescence emission intensity of activated $1'$ (in HEPES medium) upon addition of 300 μL of 10 mM 3-NTyr in presence of 300 μL of 10 mM creatinine solution ($\lambda_{\text{ex}} = 325 \text{ nm}$ and $\lambda_{\text{em}} = 428 \text{ nm}$).

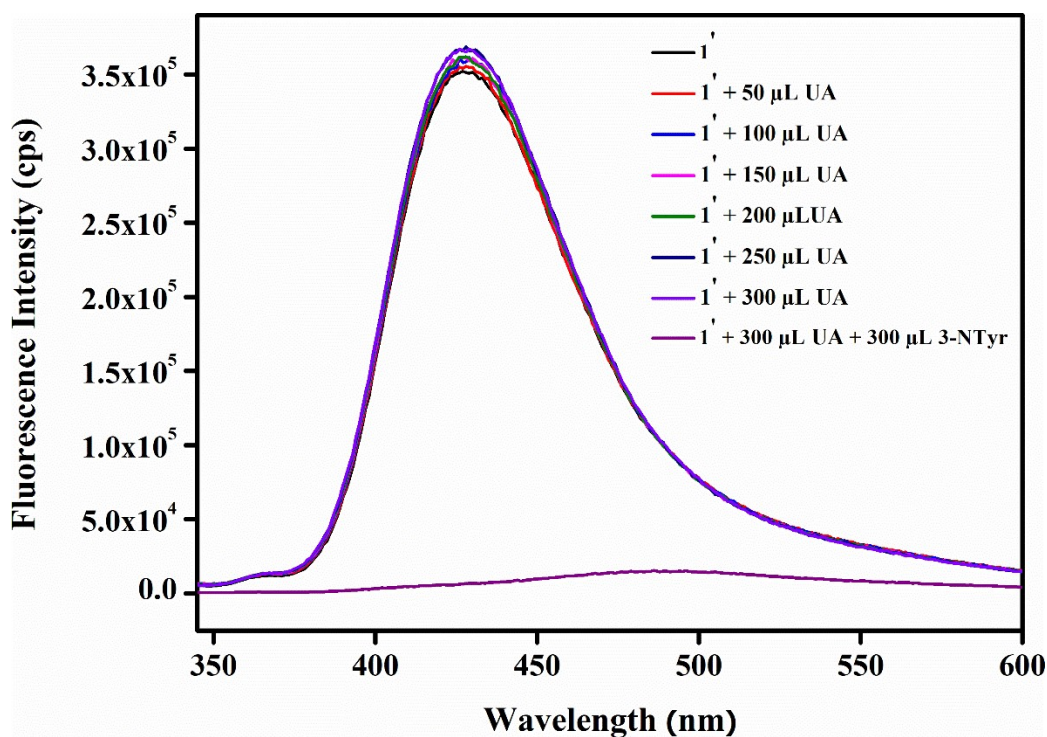


Figure S32. Change in fluorescence emission intensity of activated $1'$ (in HEPES medium) upon addition of 300 μL of 10 mM 3-NTyr in presence of 300 μL of 10 mM uric acid (UA) solution ($\lambda_{\text{ex}} = 325 \text{ nm}$ and $\lambda_{\text{em}} = 428 \text{ nm}$).

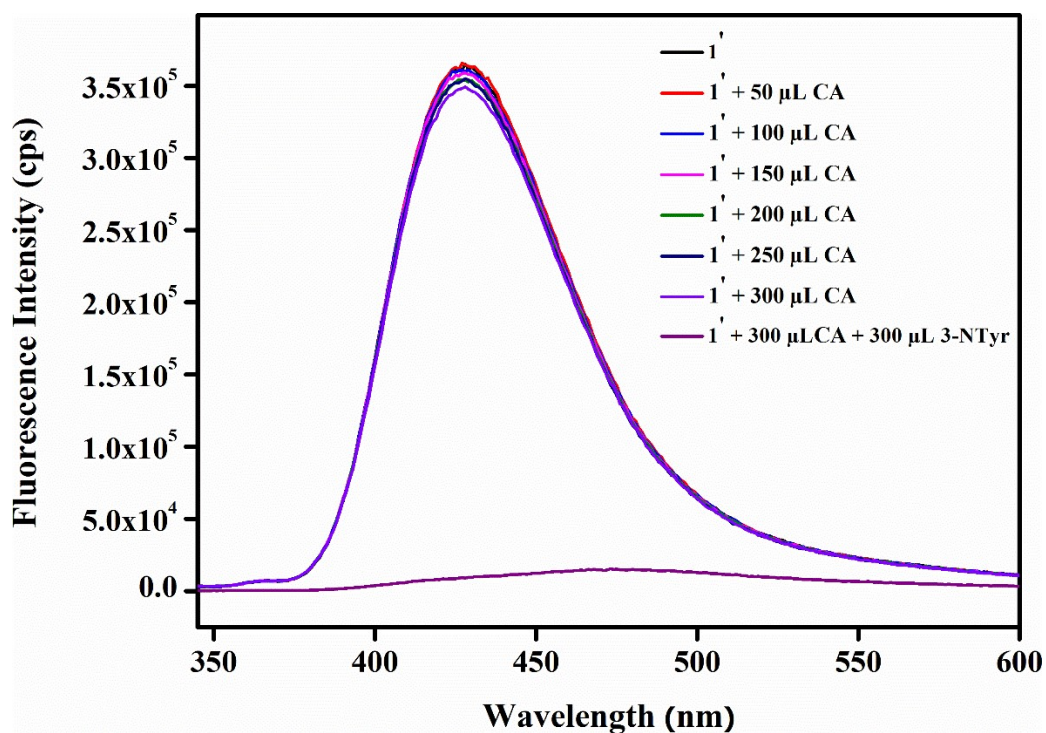


Figure S33. Change in fluorescence emission intensity of activated $1'$ (in HEPES medium) upon addition of 300 μL of 10 mM 3-NTyr in presence of 300 μL of 10 mM citric acid (CA) solution ($\lambda_{\text{ex}} = 325 \text{ nm}$ and $\lambda_{\text{em}} = 428 \text{ nm}$).

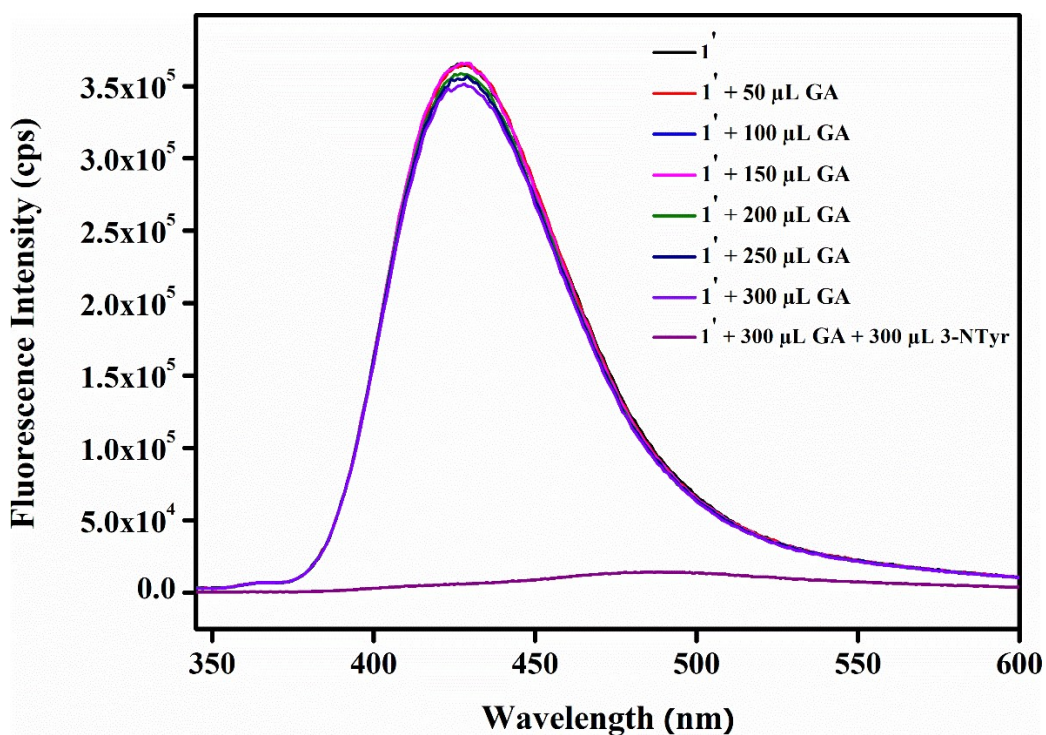


Figure S34. Change in fluorescence emission intensity of activated $1'$ (in HEPES medium) upon addition of 300 μL of 10 mM 3-NTyr in presence of 300 μL of 10 mM glutamic acid (GA) solution ($\lambda_{\text{ex}} = 325 \text{ nm}$ and $\lambda_{\text{em}} = 428 \text{ nm}$).

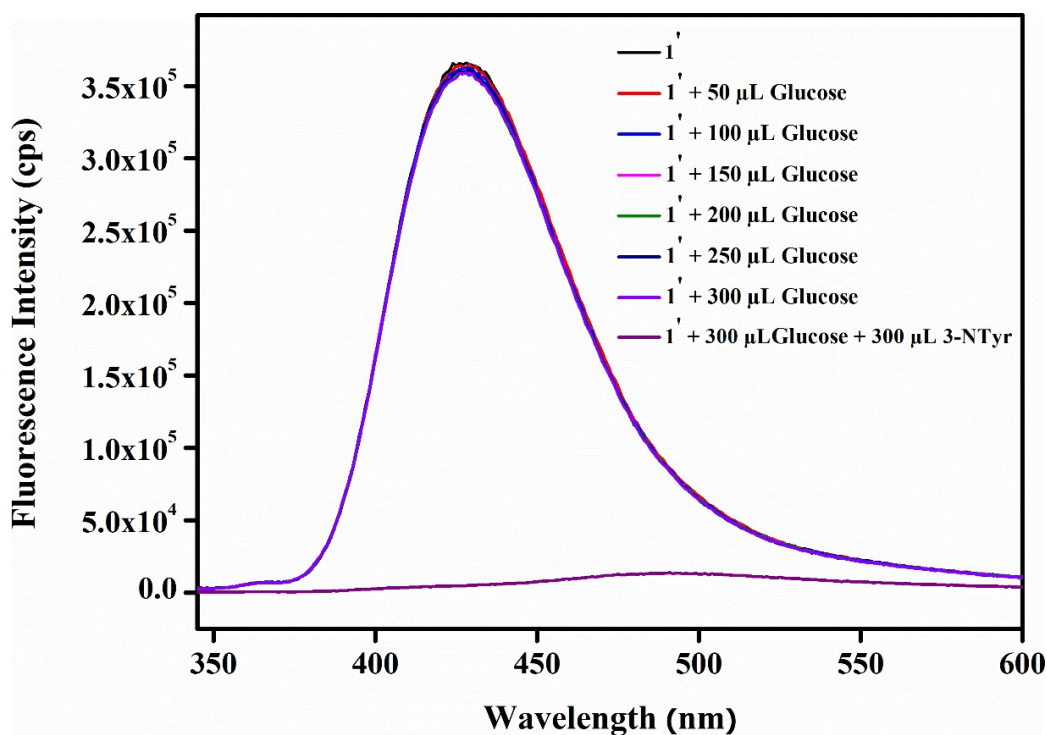


Figure S35. Change in fluorescence emission intensity of activated $1'$ (in HEPES medium) upon addition of 300 μL of 10 mM 3-NTyr in presence of 300 μL of 10 mM glucose solution ($\lambda_{\text{ex}} = 325$ nm and $\lambda_{\text{em}} = 428$ nm).

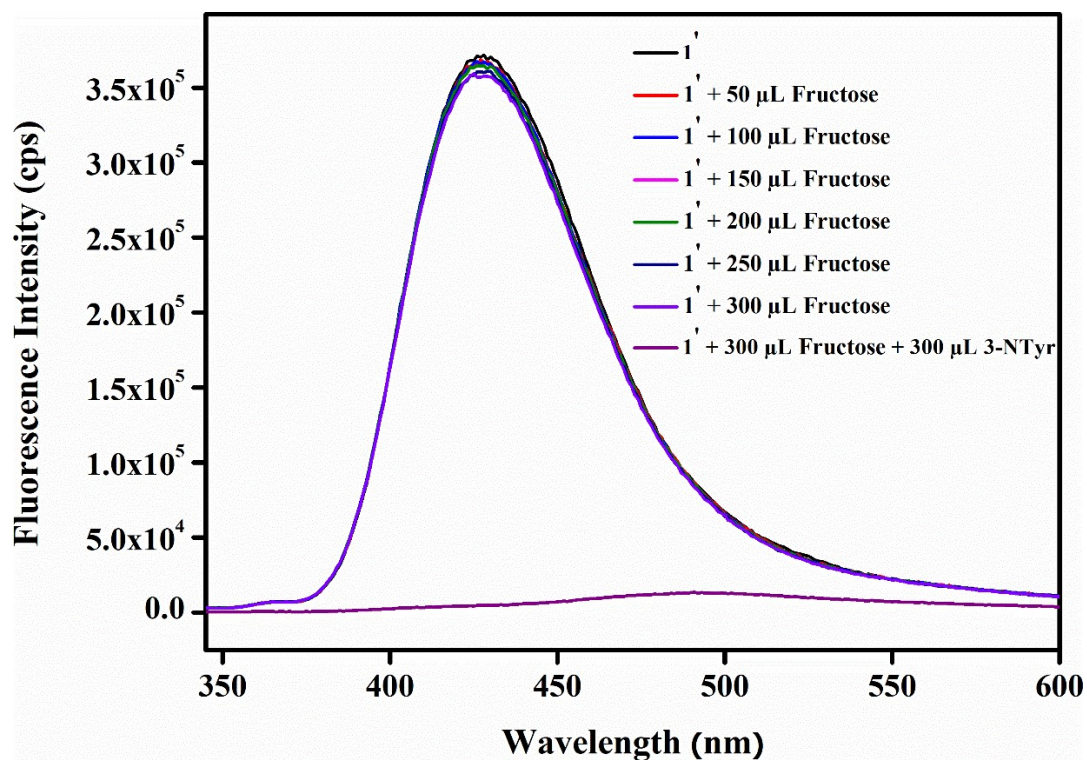


Figure S36. Change in fluorescence emission intensity of activated $1'$ (in HEPES medium) upon addition of 300 μL of 10 mM 3-NTyr in presence of 300 μL of 10 mM fructose solution ($\lambda_{\text{ex}} = 325$ nm and $\lambda_{\text{em}} = 428$ nm).

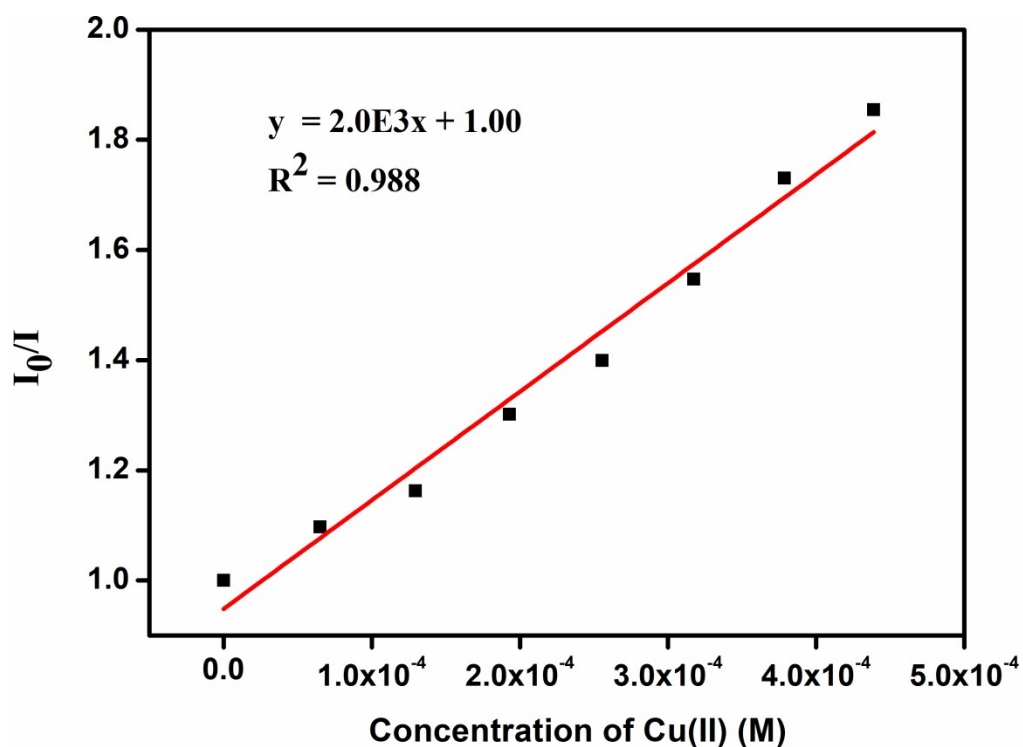


Figure S37. Stern-Volmer plot for fluorescence quenching of activated $1'$ in HEPES medium against increasing concentration of Cu^{2+} .

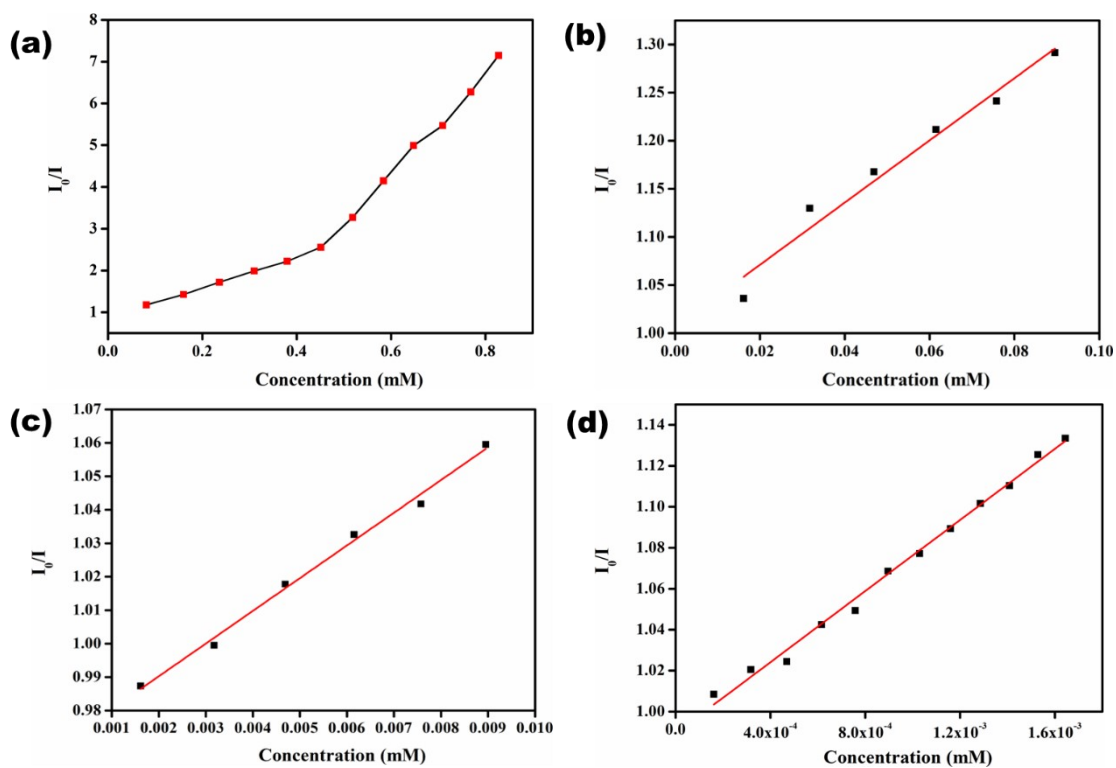


Figure S38. Stern-Volmer fluorescence quenching plot of activated $1'$ in HEPES medium against increasing different concentrations of Cu^{2+} .

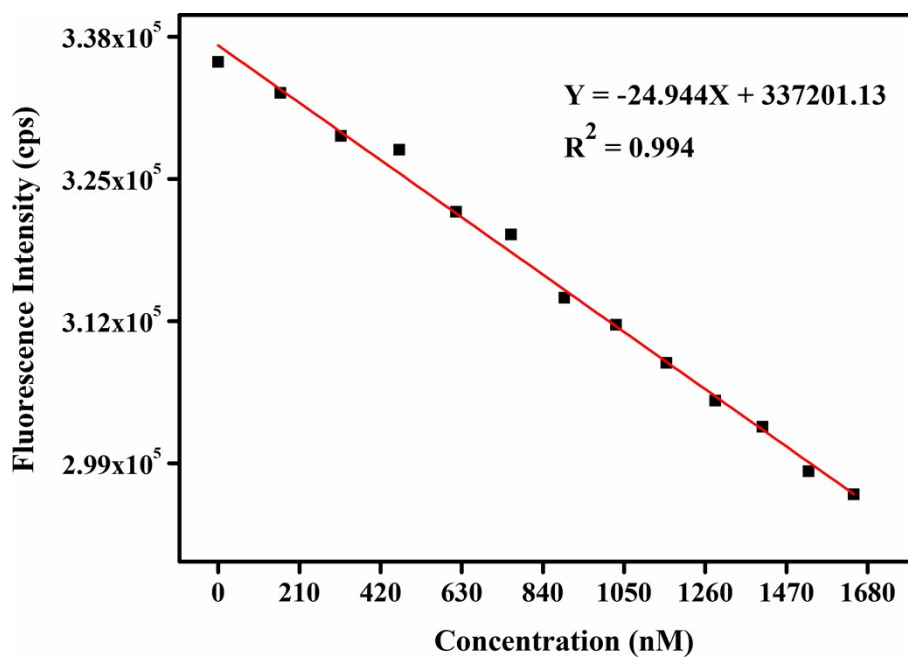


Figure S39. Change in fluorescence emission intensity of activated **1'** in HEPES medium as a function of Cu^{2+} concentration.

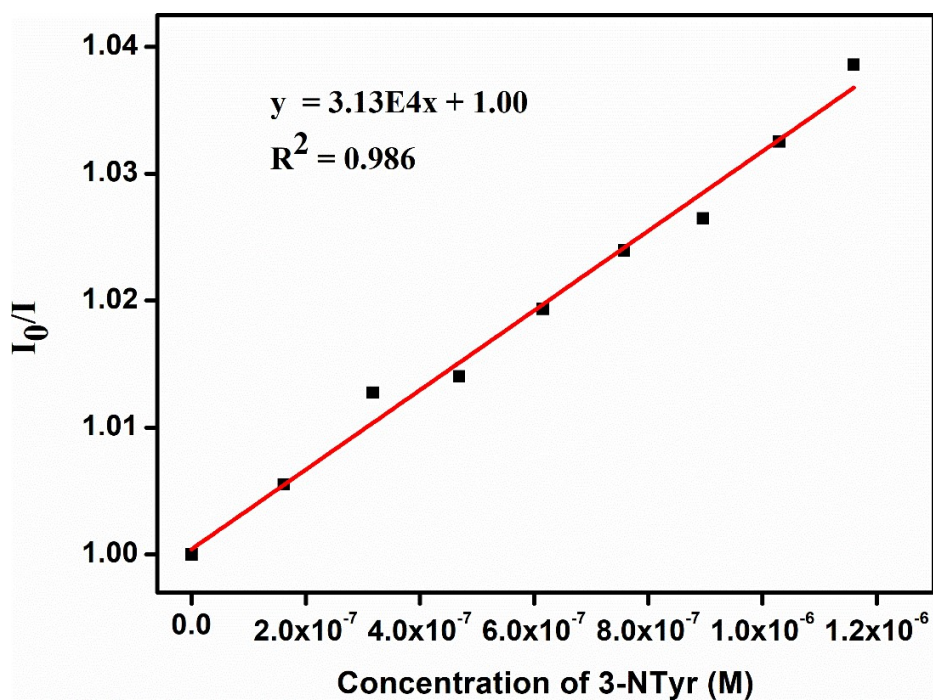


Figure S40. Stern-Volmer plot for fluorescence quenching of activated **1'** in HEPES medium against increasing concentration of 3-NTyr.

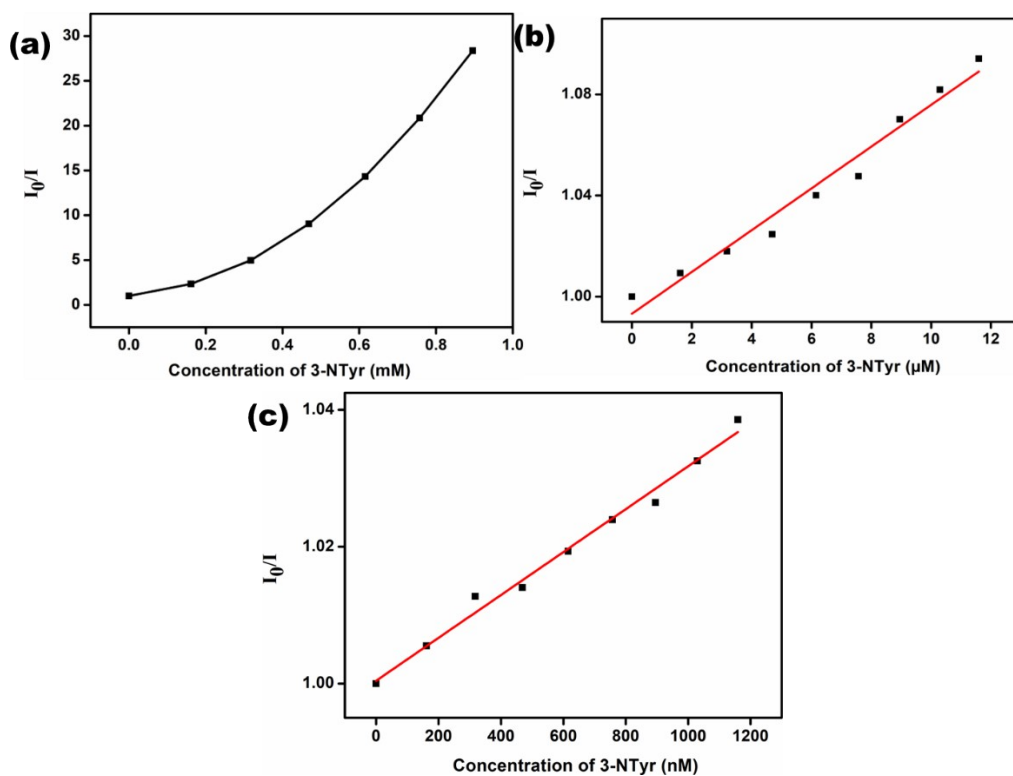


Figure S41. Stern-Volmer fluorescence quenching plot of activated **1'** in HEPES medium against increasing different concentrations of 3-NTyr.

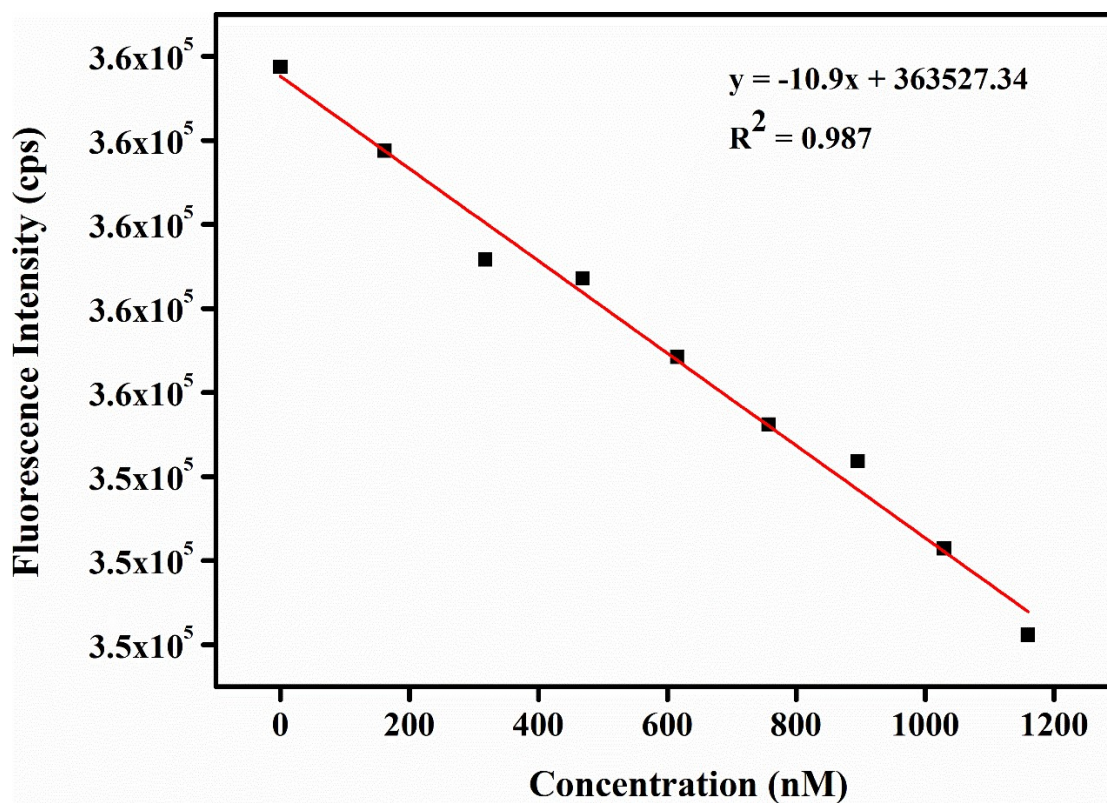


Figure S42. Change in fluorescence emission intensity of activated **1'** in HEPES medium as a function of 3-NTyr concentration.

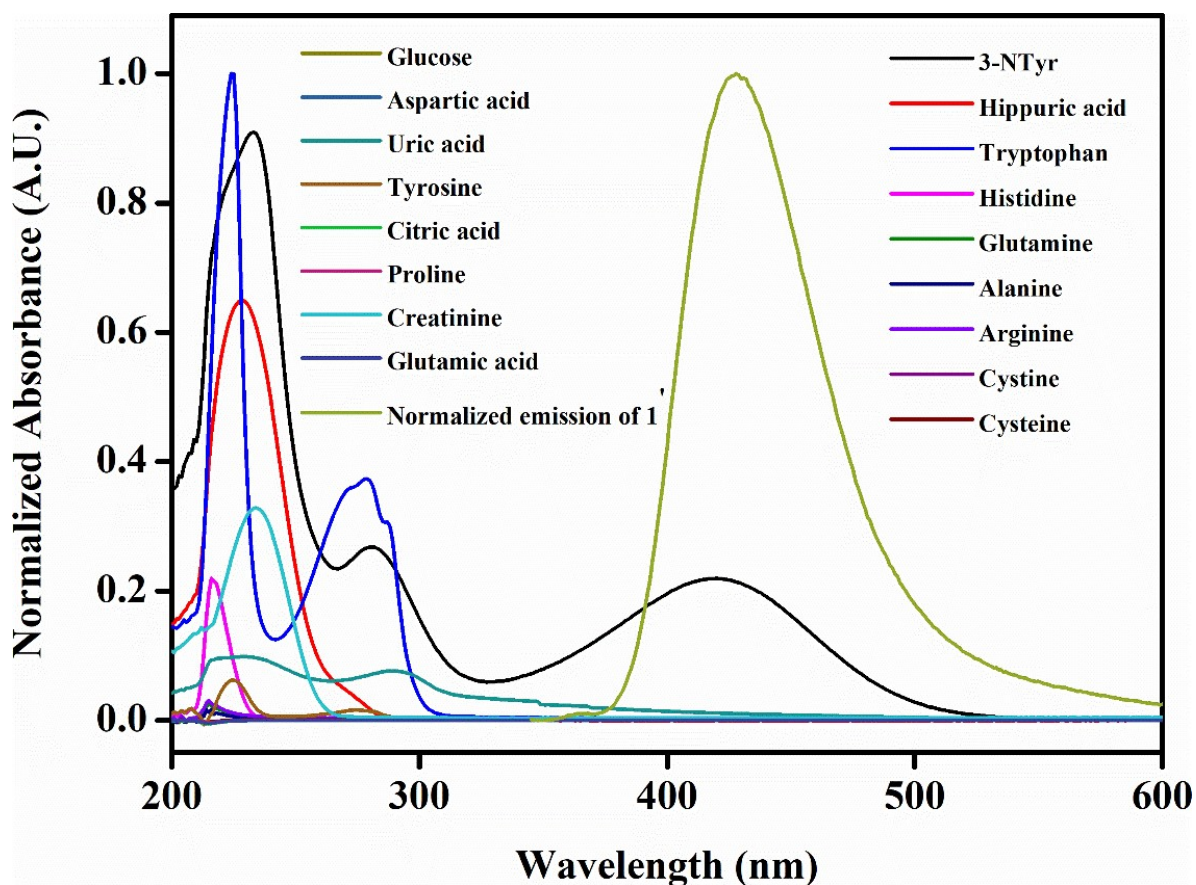


Figure S43. UV-Vis absorption spectra of all analytes and emission spectra of 1' MOF.

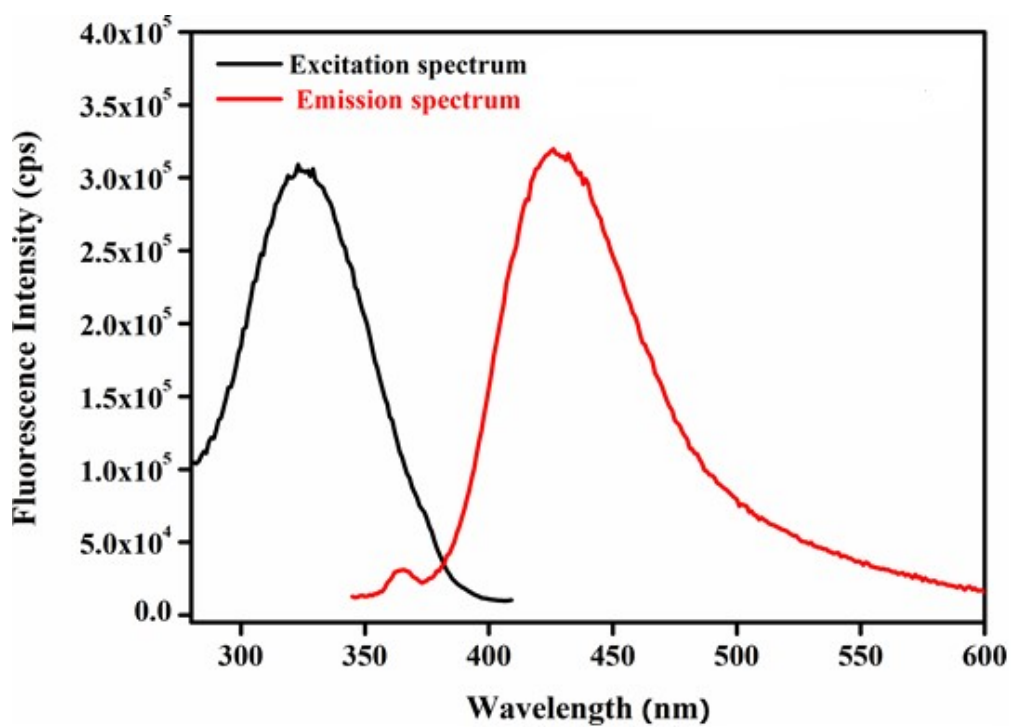


Figure S44. Excitation (red) and emission (black) spectra of 1' in HEPES buffer medium.

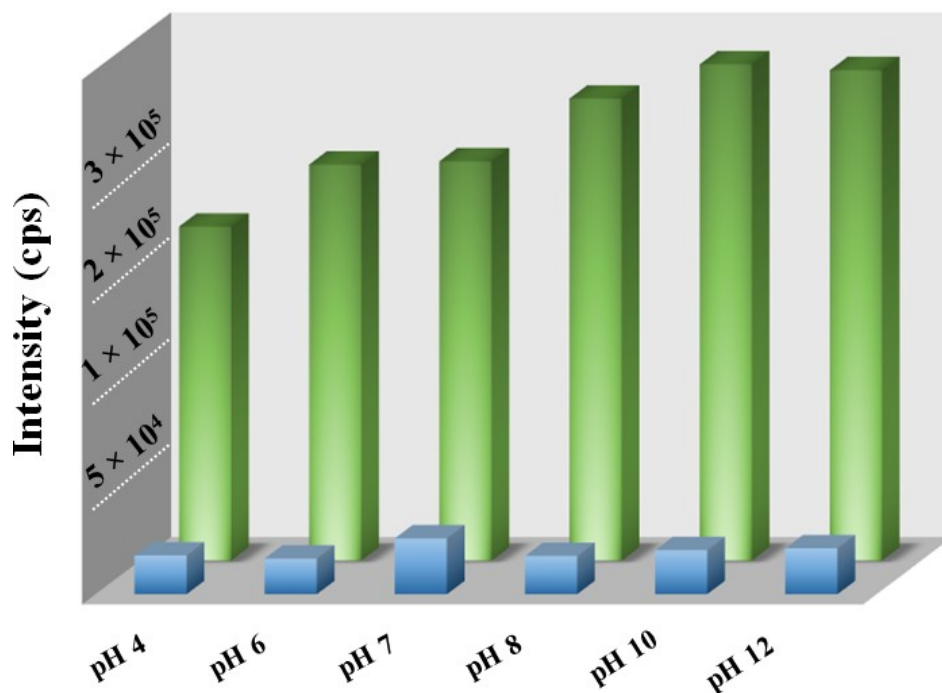


Figure S45. Quenching of fluorescence emission intensity of activated **1'** (green) and after introduction of Cu²⁺ (5 mM, 300 μ L) (blue) in different pH media.

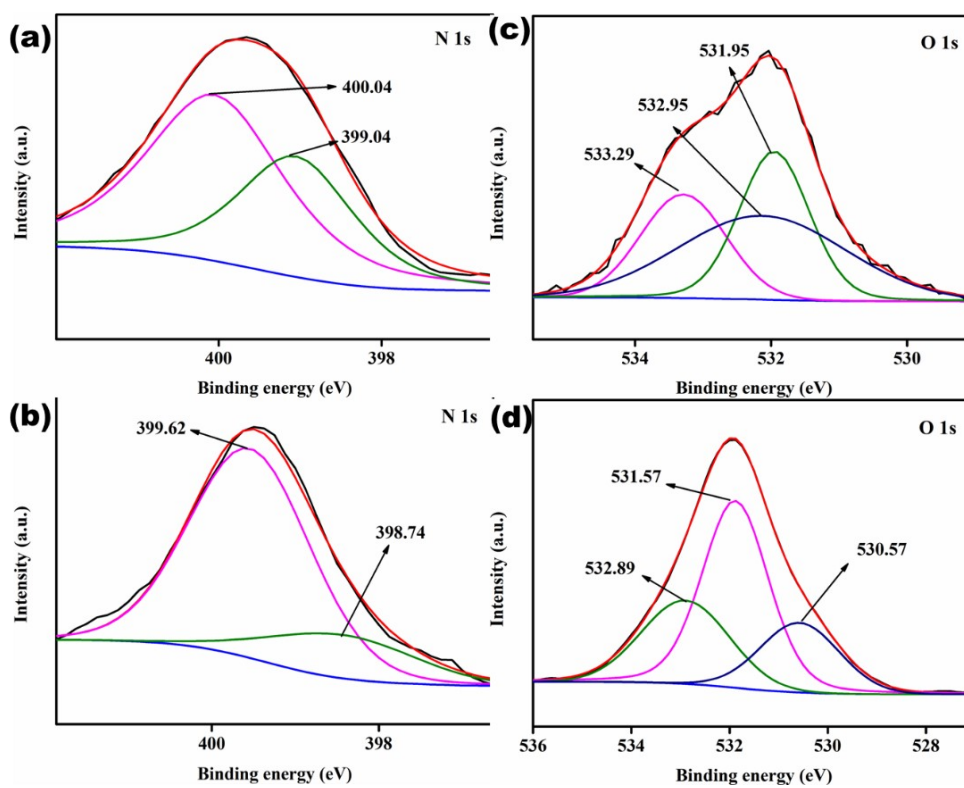


Figure S46. Fitted XPS spectra of (a) N (1s) and (c) O (1s) of **1'**. Fitted XPS spectra of (b) N (1s) and (d) O (1s) of **1'** after treatment with Cu²⁺.

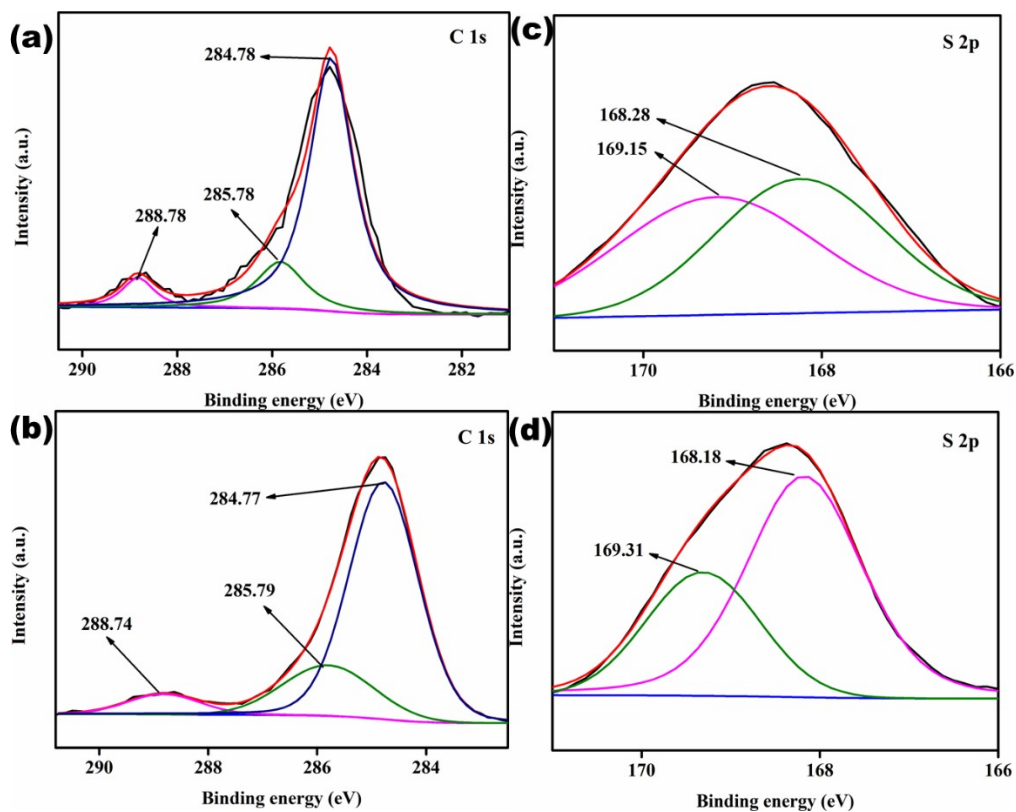


Figure S47. Fitted XPS spectra of (a) C (1s) and (c) S (2p) of **1'**. Fitted XPS spectra of (b) C (1s) and (d) S (2p) of **1'** after treatment with Cu^{2+} .

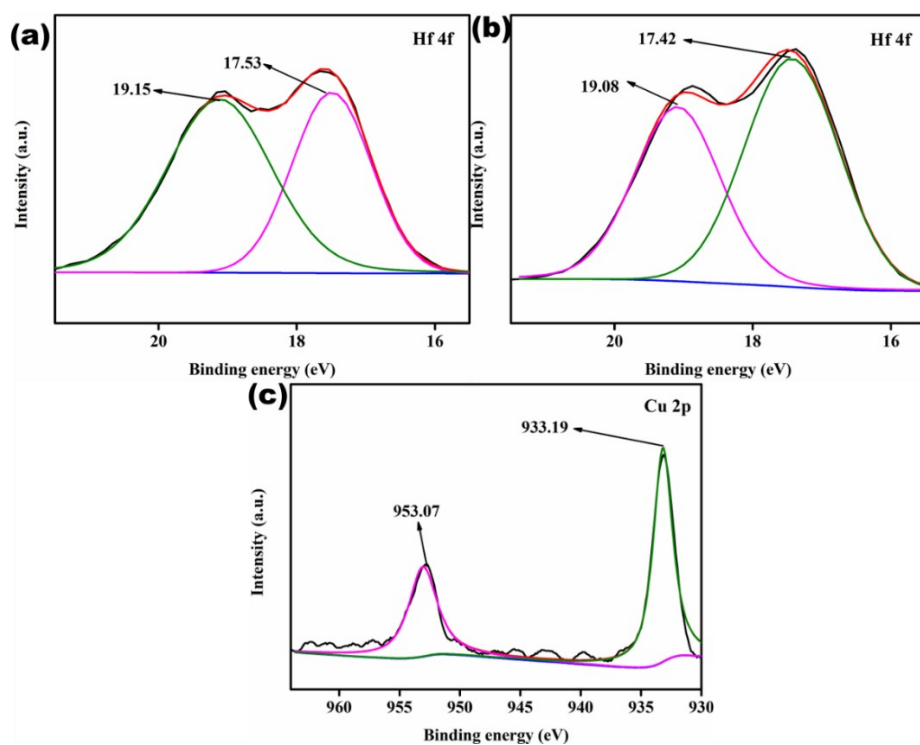


Figure S48. Fitted XPS spectra of (a) Hf (4f) of **1'**. Fitted XPS spectra of (b) Hf (4f) and (c) C (2p) of **1'** after treatment with Cu^{2+} .

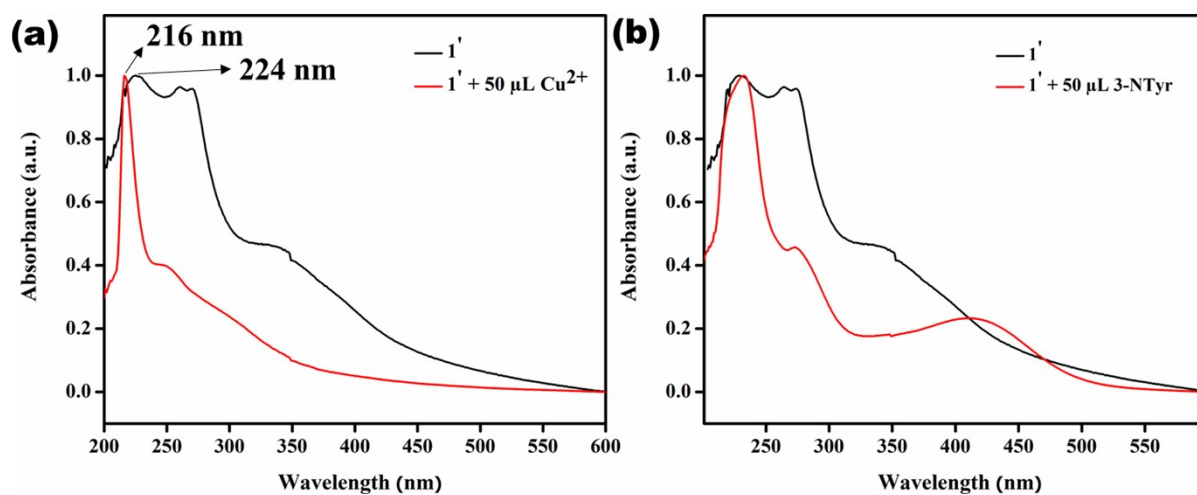


Figure S49. (a) UV-Vis spectra of **1'** in absence (black) and presence (red) of Cu^{2+} . (b) UV-Vis spectra of **1'** in absence (black) and presence (red) of 3-NTyr.

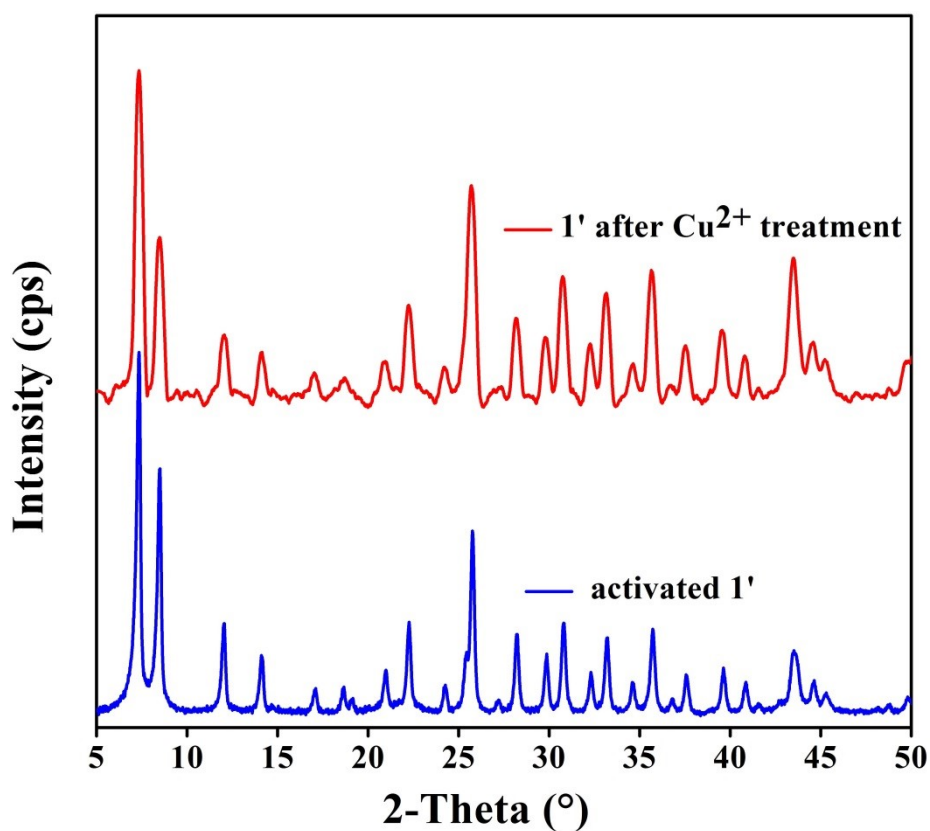


Figure S50. PXRD patterns of **1'** before (blue) and after (red) treatment with Cu^{2+} solution.

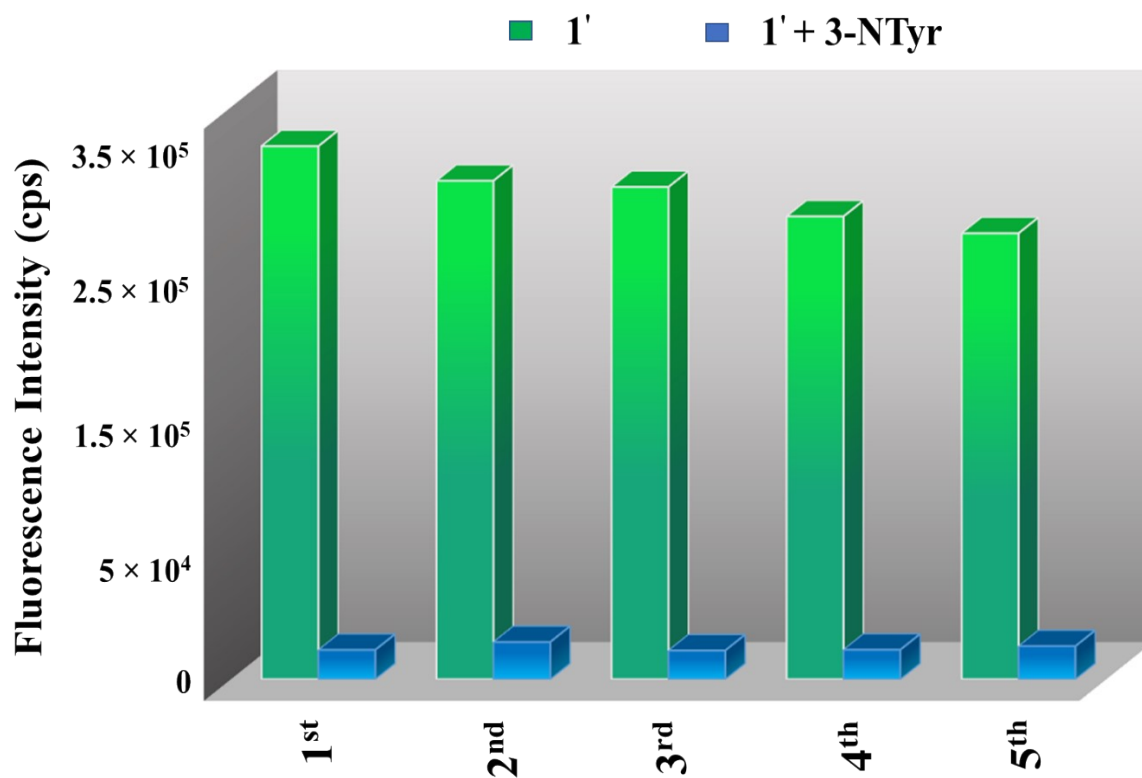


Figure S51. Recyclability experiment for detection of 3-NTyr by $1'$ in HEPES medium.

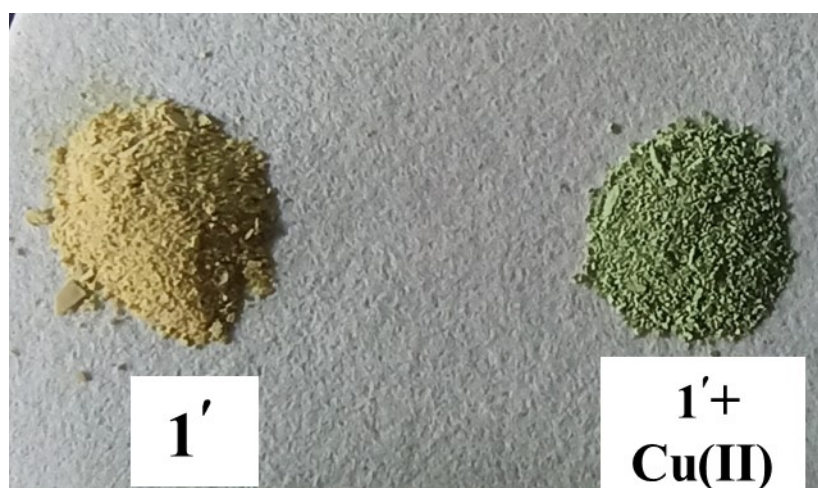


Figure S52. Digital images of $1'$ MOF and $1'$ after Cu(II) treatment.

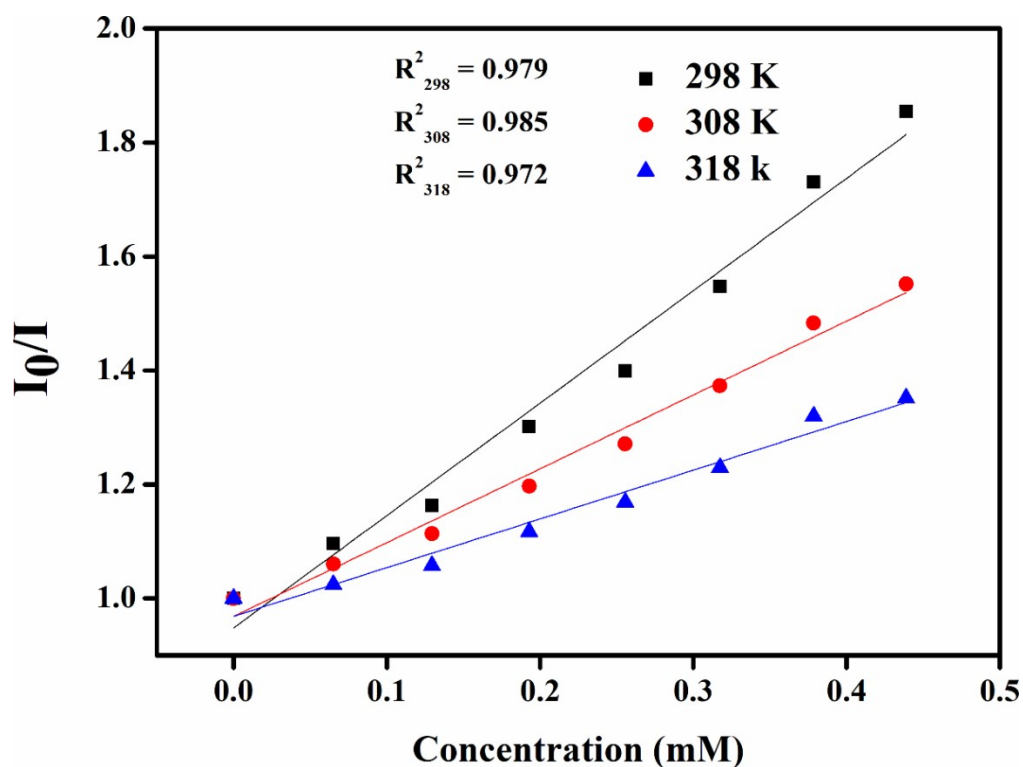


Figure S53. Stern-Volmer plots for the fluorescence emission quenching of $1'$ in presence of Cu(II) ion solution at different temperatures.

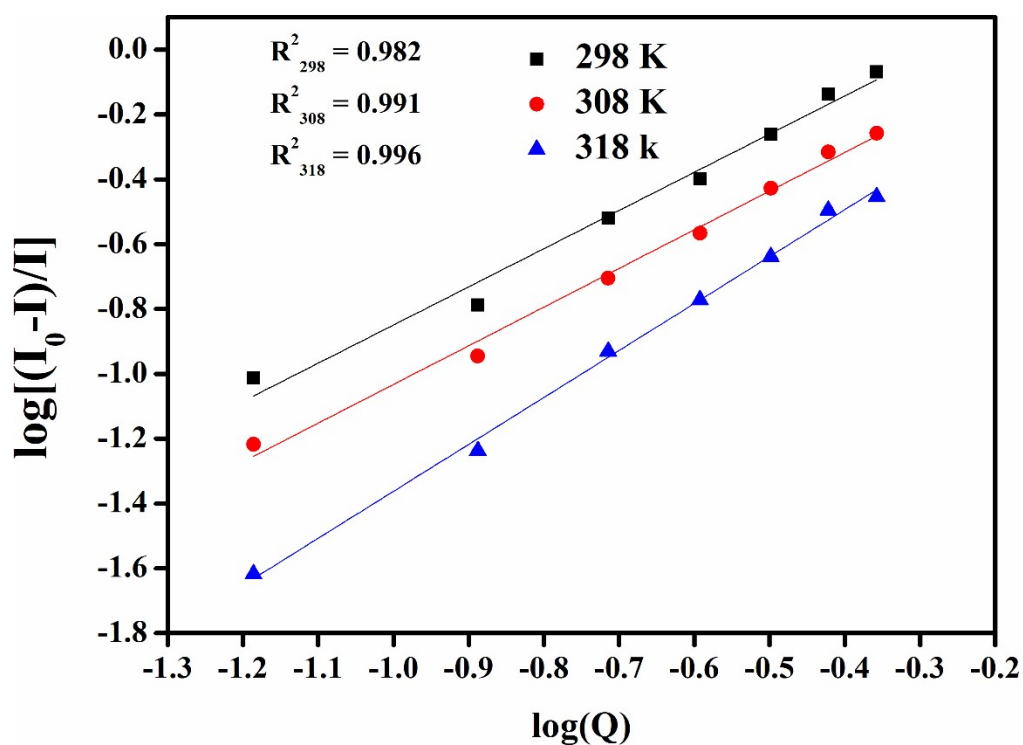


Figure S54. $\log[(I_0-I)/I]$ vs $\log(Q)$ plot at different temperatures.

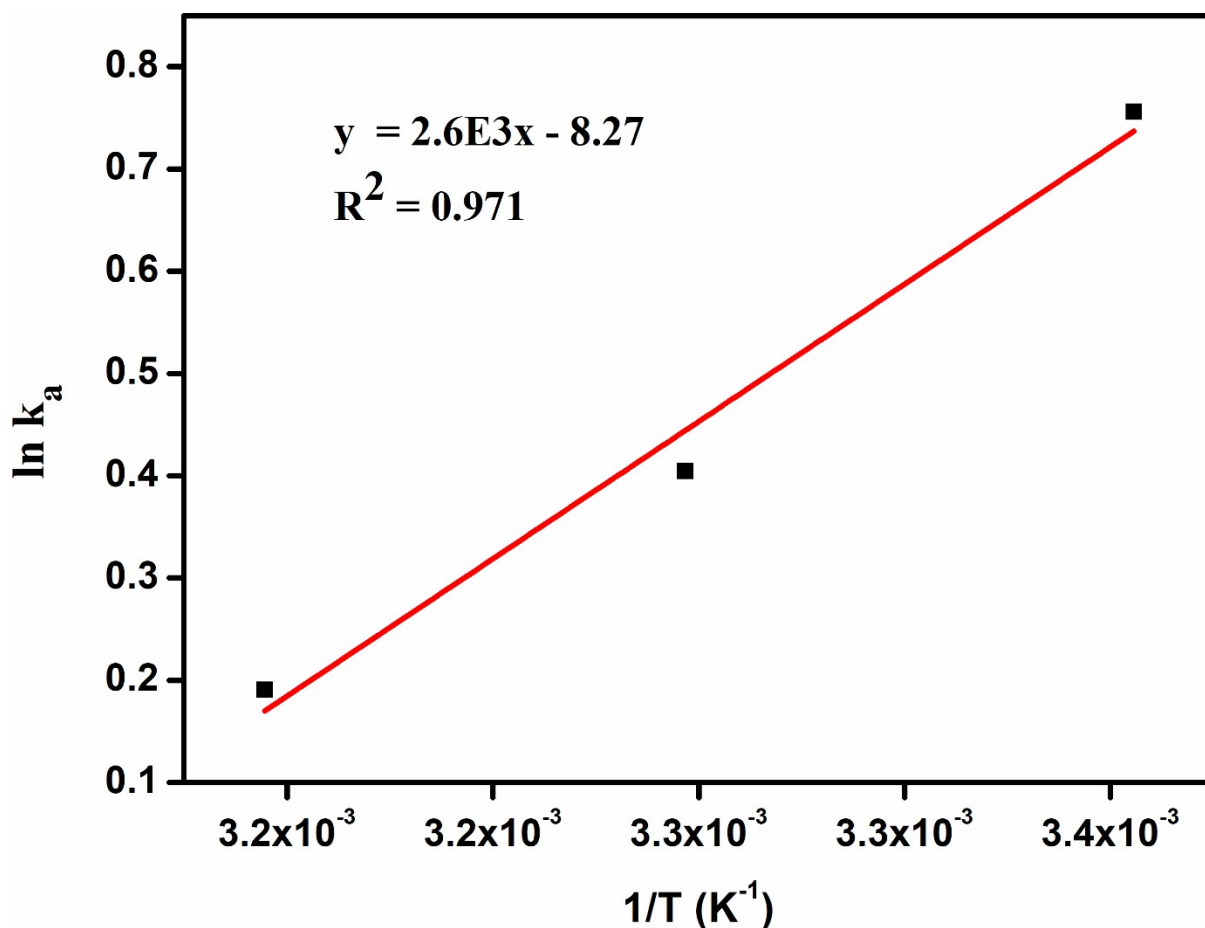


Figure S55. Van't Hoff plot for interaction of $1'$ with Cu(II) ion.

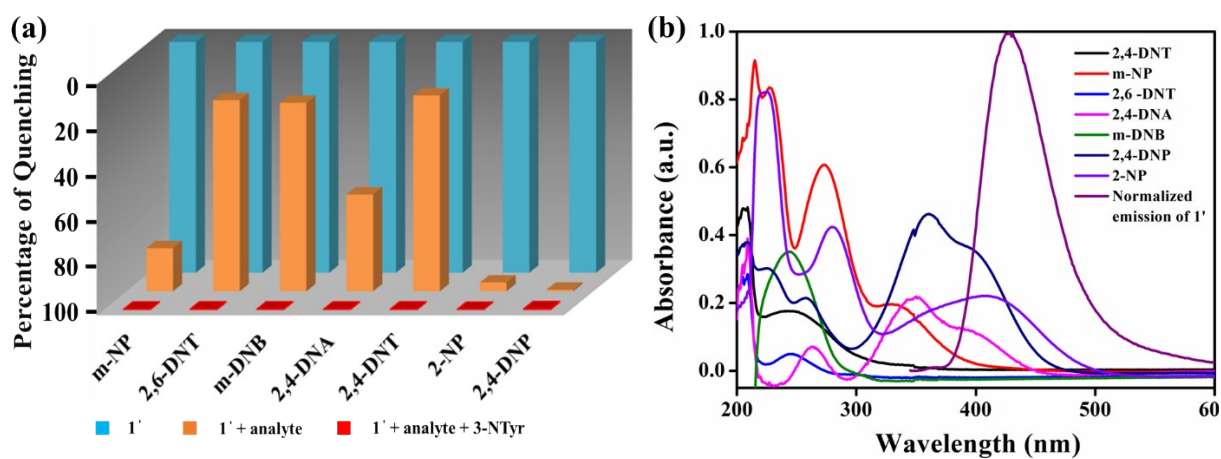


Figure S56. (a) Percentage of quenching of the fluorescence intensity of $1'$ after introduction of 3-Ntyr (10 mM, 300 μ L) in presence of different nitroaromatic compounds (10 mM, 300 μ L). (b) UV-Vis absorption spectra of nitroaromatic compounds and emission spectrum of $1'$ MOF.

Table S1. Stern–Volmer quenching constants, binding parameters and thermodynamic parameters for the binding process between **1'** and Cu(II) ion.

T (k)	$K_{SV} \times 10^3$ (Lmol ⁻¹)	$K_a \times 10^3$ (Lmol ⁻¹)	ΔG (KJmol ⁻¹)	ΔH (KJmol ⁻¹)	ΔS (mol ⁻¹ K ⁻¹)
298	2.0	2.13	-1842.5	- 22.33	- 68.75
308	1.29	1.44	-1155.0		
318	0.85	1.21	-467.5		

Table S2. Detection of Cu²⁺ in human urine samples.

Sample	Background (mol L ⁻¹)	Cu(II) Spiked (μM)	Cu ²⁺ Found (μM)	Recovery (%)	RSD (%) (n=3)
Urine	1.63 × 10 ⁶	6.15	6.26 ± 0.24	101.93 ± 4.85	4.85
		8.95	9.17 ± 0.18	102.55 ± 2.56	2.56
Serum	1.09 × 10 ⁶	6.39	6.39 ± 0.16	100.12 ± 3.54	3.54
		8.95	9.06 ± 0.18	101.08 ± 2.33	2.33

* Excluding background.

Table S3. Detection of 3-NTyr in human blood serum and urine samples.

Sample	Background (mol L ⁻¹)	3-NTyr Spiked (μM)	3-NTyr Found (μM)	Recovery (%)	RSD (%) (n=3)
Urine	1.63 × 10 ⁶	6.15	6.20 ± 0.20	100.91 ± 3.73	3.73
		8.95	9.21 ± 0.15	102.90 ± 2.11	2.11
Serum	1.09 × 10 ⁶	6.15	6.16 ± 0.18	103.98 ± 3.26	3.26
		8.95	9.04 ± 0.17	101.07 ± 2.31	2.31

* Excluding background.

Table S4. Detection of Cu²⁺ in different environmental water samples.

Sample	Spiked Concentration (M)	Recovered Concentration	Recovery Percentage
Distilled water	49 × 10 ⁻⁵	47 × 10 ⁻⁵	96.38
Lake water		49 × 10 ⁻⁵	101.67
River water		46 × 10 ⁻⁵	94.67
Tap water		50 × 10 ⁻⁵	103.95

Table S5. Fluorescence lifetime of **1'** before and after addition of Cu(II) ($\lambda_{ex} = 336$ nm), pulsed diode laser).

Sample	a_1	τ_1 (ns)	$\langle \tau \rangle^*$ (ns)	χ^2
--------	-------	---------------	-------------------------------	----------

1'	1	14.1	14.1	1.007
1' + Cu(II)	1	13.9	13.9	1.000
1' + 3-NTyr	1	10.9	10.9	1.024

Average lifetime $\langle \tau \rangle^* = a_1 \tau_1$

Table S6. Comparison of various MOF-based probes previously reported in the literature for the fluorometric detection of Cu²⁺.

Sl. No.	Sensor Material	Sensing Medium	Response Time	LOD	Ref.
1	MOF 1'	HEPES buffer	< 10 s	229 nM	this work
2	Cd-MOF-74	water and HEPES	10 min	78.7 μ M	3
3	{[Nd ₂ (NH ₂ -BDC) ₃ (DMF) ₄]} _n	DMF	-	24.95 μ M	4
4	[Eu(pdc) _{1.5} (DMF)]·(DMF) _{0.5} (H ₂ O) _{0.5}	DMF	30 min	10 μ M	5
5	UiO-66-NH ₂	water	-	2.5 μ M	6
6	[ZnL ₂] _n	water	-	1 μ M	5
7	[Eu(HL)(L)(H ₂ O) ₂]·2H ₂ O	Water	-	10 μ M	7
8	[NH ₄] ₂ [ZnL]·6H ₂ O	water	-	1 μ M	8
9	Zn(MeIM) ₂ ·(DMF)·(H ₂ O) ₃	solid phase	-	1 mM	9
10	[Cd(2-aip)(bpy)]·2DMF	DMF	10s	10 mM	10
11	Zr-BPDC-(SO ₃ H) ₂	acetonitrile	15 s	0.22 μ M	11
12	MIL-53-L	water	-	10 μ M	12
13	{[Mg ₃ (ndc) _{2.5} (HCO ₂) ₂ (H ₂ O)][NH ₂ Me ₂]·2H ₂ O·DMF}	ethanol	>7 days	10 μ M	13
14	{NH ₂ (CH ₃) ₂ ·Cd _{2.5} (L) ₂ (H ₂ O)·(H ₂ O)} _n	water	9 s	0.1 mM	14
15	MOF-525	DMF	40 s	67 nM	15

Table S7. Comparison of various probes previously reported in the literature for the fluorometric detection of 3-NTyr.

Sl. No.	Sensor Material	Type of Material	Sensing Medium	Response Time	LOD	Ref.
1	MOF 1'	MOF	HEPES buffer	< 10 s	539 nM	this work
2	[Zn(L)(HBTC)]	MOF	water	24 s	310 nM	16
3	TPE	organic	water	-	3 μ M	17

		molecules				
4	CDs	carbon dots	MES buffer	-	34 μ M	18
5	BMIP@CDs	CD@MOF	Phosphate buffer	8 min	17 nM	19

References:

1. S. Mukherjee, S. Ghosh and S. Biswas, *Inorg. Chem. Front.*, 2022, **9**, 6288-6298.
2. S. Nandi and S. Biswas, *Microporous Mesoporous Mater.*, 2020, **299**, 110116.
3. T.-T. Zheng, J. Zhao, Z.-W. Fang, M.-T. Li, C.-Y. Sun, X. Li, X.-L. Wang and Z.-M. Su, *Dalton Trans.*, 2017, **46**, 2456-2461.
4. J. Luo, B. S. Liu, C. Cao and F. Wei, *Inorg. Chem. Commun.*, 2017, **76**, 18-21.
5. B. Liu, L. Hou, W.-P. Wu, A.-N. Dou and Y.-Y. Wang, *Dalton Trans.*, 2015, **44**, 4423-4427.
6. L. Wu, X.-F. Zhang, Z.-Q. Li and F. Wu, *Inorg. Chem. Commun.*, 2016, **74**, 22-25.
7. L.-N. Zhang, A.-L. Liu, Y.-X. Liu, J.-X. Shen, C.-X. Du and H.-W. Hou, *Inorg. Chem. Commun.*, 2015, **56**, 137-140.
8. S. Liu, J. Li and F. Luo, *Inorg. Chem. Commun.*, 2010, **13**, 870-872.
9. S. Liu, Z. Xiang, Z. Hu, X. Zheng and D. Cao, *J. Mater. Chem.*, 2011, **21**, 6649-6653.
10. H.-N. Wang, P.-X. Liu, H. Chen, N. Xu, Z.-Y. Zhou and S.-P. Zhuo, *RSC Adv.*, 2015, **5**, 65110-65113.
11. A. Rana, S. Nandi and S. Biswas, *New J. Chem.*, 2022, **46**, 10477-10483.
12. C. Liu and B. Yan, *Sens. Actuators B: Chem.*, 2016, **235**, 541-546.
13. S. Bhattacharyya, A. Chakraborty, K. Jayaramulu, A. Hazra and T. K. Maji, *Chem. Commun.*, 2014, **50**, 13567-13570.
14. C. Qiao, X. Qu, Q. Yang, Q. Wei, G. Xie, S. Chen and D. Yang, *Green Chem.*, 2016, **18**, 951-956.
15. L. Li, S. Shen, R. Lin, Y. Bai and H. Liu, *Chem. Commun.*, 2017, **53**, 9986-9989.
16. J. Geng, Y. Li, H. Lin, Q. Liu, J. Lu and X. Wang, *Dalton trans.*, 2022, **51**, 11390-11396.
17. L. A. Pérez-Márquez, M. D. Perretti, R. García-Rodríguez, F. Lahoz and R. Carrillo, *Angew. Chem. Int. Ed.*, 2022, **61**, e202205403.
18. N. Camilus, S. Gao, M. Mitti, J.-R. Macairan, R. Naccache and S. Martic, *Spectrochim. Acta A Mol. Biomol. Spectrosc.*, 2022, 121444.
19. R. Jalili and M. Amjadi, *Sens. Actuators B Chem.*, 2018, **255**, 1072-1078.